

**Development of zebrafish embryo model, an  
alternative *in vivo* vertebrate system for radiation  
biology research**

Ph.D. Thesis

**Emília Rita Szabó**

Doctoral School of Clinical Medicine  
Department of Oncotherapy  
University of Szeged, Faculty of Medicine

Supervisor:

**Katalin Hideghéty M.D., Ph.D., Habil.**

Extreme Light Infrastructure - Attosecond Light Pulse Source  
ELI-HU Non-Profit Ltd.

Szeged

2018

### Original publications directly related to the thesis

- I.** Szabó E R, Plangár I, Tőkés T, Mán I, Polanek R, Kovács R, Fekete G, Szabó Z, Csenki Zs, Baska F, Hideghéty K. (2016) L-alpha glycerylphosphorylcholine as a Potential Radioprotective Agent in Zebrafish Embryo Model. *Zebrafish* 13: 481-488.  
**IF. 2.242**
- II.** Szabó E R, Reisz Z, Polanek R, Tőkés T, Czifrus Sz, Pesznyák Cs, Biró B, Fenyvesi A, Király B, Molnár J, Daroczi B, Szabó Z, Brunner Sz, Varga Z, Hideghéty K. (2018) A novel vertebrate system for the examination and direct comparison of the relative biological effectiveness for different radiation qualities and sources. *Int J Radiat Biol*  
**IF. 1.99**
- III.** Szabó E R, Tőkés T, Polanek R, Pesznyák Cs, Czifrus Sz, Hideghéty K. (2018) Gerinces modell alkalmazása különböző sugárminőségek relatív biológiai effektivitásának tesztelésére. *Eötvös Lóránd Fizikai Társulat Sugárvédelmi Szakcsoportjának On-line folyóirata*
- IV.** Szabó E R, Brand M, Hans S, Hideghéty K, Karsch L, Leßmann E, Pawelke J, Schürer M, Beyreuther E. (2018) Radiobiological effects and proton RBE determined by wildtype zebrafish embryos. *Plos One* (under review)  
**IF. 2.806**

**Total impact factor: 7.038**

### Publications not directly related to the thesis

- I.** Hideghéty K, Plangár I, Mán I, Fekete G, Nagy Z, Volford G, Tőkés T, Szabó E, Szabó Z, Brinyiczki K, Mózes P, Németh I. (2013) Development of a small-animal focal brain irradiation model to study radiation injury and radiation-injury modifiers. *Int J Radiat Biol* 89: 645–655.  
**IF: 1.895**
- II.** Plangár I, Szabó ER, Tőkés T, Mán I, Brinyiczki K, Fekete G, Németh I, Ghyczy M, Boros M, Hideghéty K. (2014) Radio-neuroprotective effect of L-alpha-glycerylphosphorylcholine (GPC) in an experimental rat model. *J Neurooncol* 119: 253-61.  
**IF. 3.51**

- III.** Tőkés T, Varga G, Garab D, Nagy Z, Fekete G, Tuboly E, Plangár I, Mán I, **Szabó RE**, Szabó Z, Volford G, Ghyczy M, Kaszaki J, Boros M, Hideghéty K. (2014) Peripheral inflammatory activation after hippocampus irradiation in the rat. *Int J Radiat Biol* 90: 1-6  
**IF.1.895**
- IV.** Mán I, Szebeni GJ, Plangár I, **Szabó ER**, Tőkés T, Szabó Z, Nagy Z, Fekete G, Fajka-Boja R, Puskás LG, Hideghéty K, Hackler L Jr. (2015) Novel real-time cell analysis platform for the dynamic monitoring of ionizing radiation effects on human tumor cell lines and primary fibroblasts. *Mol Med Rep* 12: 4610-4619.  
**IF.1.559**
- V.** Hideghéty K, **Szabó E R**, Polanek R, Szabó Z, Brunner Sz, Tőkés T. (2017) New approaches in clinical application of laser-driven ionizing radiation. *Spie Optics+ Optoelectronics Proceedings* vol. 10239
- VI.** Hideghéty K, **Szabó E R**, Polanek R, Szabó Z, Ughy B, Brunner Sz, Tőkés T. (2017) An evaluation of the various aspects of the progress in clinical applications of laser driven ionizing radiation. *Journal of Instrumentation*, vol. 12  
**IF.1.22**
- VII.** Beyreuther E, Brüchner K, Krause M, Schmidt M, **Szabó E R**, Pawelke J. (2017) An optimized small animal tumour model for experimentation with low energy protons. *PLoS One* 18; 12(5):e0177428.  
**IF. 2.806**
- VIII.** Katona M, Tőkés T, **Szabó E R**, Brunner Sz, Szabó Z I, Polanek R, Hideghéty K, Nyúl L. (2018) Automatic Segmentation and Quantitative Analysis of Irradiated Zebrafish Embryos *Computational Modeling of Objects Presented in Images. Fundamentals, Methods, and Applications: Heidelberg-Berlin, Springer Verlag, Lecture Notes in Computer Science Vol. 10986*

**Total impact factor: 12.885**

**Cumulative impact factor: 19.923**

## TABLE OF CONTENTS

List of abbreviation .....	6
SUMMARY .....	8
1. Establishment of optimal parameters of the zebrafish embryo system for radiobiology .....	8
2. Research on radiation modifying agent .....	9
3. Studies on high LET neutron irradiation, determination of relative biological effectiveness (RBE) of different neutron energies .....	9
4. Examination of the biological effects of proton beam at different points of the depth dose curve (plateau, mid of spread-out Bragg Peak (SOBP)) .....	9
1. INTRODUCTION .....	11
1.1. Radiation induced damages on normal tissue .....	12
1.2. Therapeutic index .....	13
1.3. Radiation modifiers .....	14
1.3.1. Potential therapeutic effects of phosphatidylcholine .....	14
1.4. Different radiation qualities .....	15
1.4.1. Neutron irradiation .....	15
1.4.2. Proton irradiation .....	16
1.5. Zebrafish as a model system .....	17
1.6. Biological model development for research on laser driven proton sources .....	18
2. AIMS .....	20
3. MATERIAL AND METHODS .....	21
3.1. Animal model .....	21
3.2. Embryo harvesting and maintenance .....	21
3.3. Method of establishment of the zebrafish embryo model for radiobiology .....	21
3.3.1. Test organism .....	21
3.3.2. Irradiation treatment .....	22
3.3.3. Morphology and survival analysis .....	22
3.3.4. Histopathology .....	23
3.4. Studying the effects of the radiation modifier .....	23
3.4.1. GPC pre-treatment .....	23
3.4.2. Survival and morphology assessments .....	24
3.4.3. Quantitative Polymerase Chain Reaction .....	24
3.4.4. Histopathology .....	24
3.5. Method of RBE definition of different high LET sources .....	25

3.5.1. Embryos handling.....	25
3.5.2. Photon irradiation .....	25
3.5.3. Fission neutron irradiation.....	25
3.5.4. Cyclotron generated fast neutron radiation .....	26
3.5.5. Analysis of neutron treatment effects on morphology and survival.....	28
3.5.6. Histopathology and tissue morphology evaluation .....	28
3.6. Method for studying the biological effects of the charged particle beam.....	29
3.6.1. Zebrafish embryo handling and preparation.....	29
3.6.2. Setup for reproducible irradiation at horizontal beams .....	29
3.6.3. Irradiation with protons .....	30
3.6.4. Photon reference irradiation .....	31
3.6.5. Survival and morphology analysis .....	32
3.6.6. Scoring system for quantitative analysis of embryo malformations .....	32
3.6.7. Statistical analysis .....	33
4. RESULTS .....	35
4.1. Age related radiation dose-response relationship .....	35
4.1.1. Histopathology .....	36
4.2. The effects of GPC on survival and distortion.....	37
4.2.1. Histological evaluation .....	38
4.2.2. Inflammatory cytokine level measurement .....	39
4.3. Survival for high LET-RBE definition .....	40
4.3.1. RBE determination by malformation .....	41
4.3.2. Histopathology evaluation of different organs .....	42
4.3.3. Proton treatment - RBE determination .....	45
5. DISCUSSION .....	49
5.1. Age and dose dependent survival curves .....	49
5.2. Testing of potential radiation modifier .....	49
5.3. RBE determination of different high LET neutron sources .....	50
5.4. Biological effects of proton beam .....	52
6. CONCLUSION AND FINDINGS .....	54
7. ACKNOWLEDGEMENTS .....	55
8. REFERENCES.....	56
ANNEX .....	68

**List of abbreviations**

2D	2 dimensional
3D	3 dimensional
AB	inbred wild type laboratory zebrafish strain
ANOVA	analysis of variance
BBB	blood brain barrier
BNCT	boron neutron capture therapy
BPFEPT	boron proton fusion enhanced proton therapy
CDDO-TFEA	CDDO-trifluoroethyl-amide
cDNA	complementary deoxyribonucleic acid
CNS	central nervous system
CRTD	Center for Regenerative Therapies at Technische Universität Dresden
DNA	deoxyribonucleic acid
dpf	day post fertilization
dpi	day post irradiation
DSB	double strand breaks
EBRT	external beam radiotherapy
FNT	fast neutron therapy
gcl	ganglion cell layer
GPC	L-alpha glycerylphosphorylcholine
Gy	Gray
H&E	hematoxylin and eosin
hpf	hours post fertilization
IC	ionization chamber
IDL	Interactive Data Language
IL-1 $\beta$	Interleukin 1 beta
inl	inner nuclear layer
ipl	inner plexiform layer
IR	ionizing radiation
LD <sub>50</sub>	lethal dose, 50% (median lethal dose)
LDAP	laser driven accelerated particles
LDI	laser driven ionizing
LET	linear energy transfer

LINAC	linear accelerator
MD	median value
MBT	midblastula transition
MCNP	Monte Carlo transport code
MeV	megaelectron volt
mRNA	messenger ribonucleic acid
MU	monitor unit
MV	megavolt
N	number of embryos
NF- $\kappa$ B	nuclear factor kappa B
onl	outer nuclear layer
opl	outer plexiform layer
PC	phosphatidylcholine
PL	phospholipid
PMMA	polymethyl methacrylate
PT	proton therapy
qPCR	quantitative polymerase chain reaction
RBE	Relative Biological Effectiveness
RNA	ribonucleic acid
RNS	reactive nitrogen species
ROS	reactive oxygen species
rpe	retinal pigmented epithelium
rRNA	ribosomal ribonucleic acid
SD	standard deviation
SEM	standard error of the mean
SOBP	spread-out Bragg peak
SSB	single strand breaks
SSD	source to surface distance
SV	scoring values
UPTD	University Proton Therapy Dresden
VHEE	very high energy electron

## SUMMARY

Radiotherapy has consistently remained one of the most effective treatments of complex cancer management. The direct cell damaging effects of ionizing radiation (IR), the main target of which is the hereditary material, has long been known. Radiation biology research has led to a significant improvement in effective cancer cell killing and the preservation of normal tissue function, resulting in an improvement in the therapeutic index. The recent rapid increase of hadron therapy applications requires the development of high performance, reliable *in vivo* models for preclinical research on the biological effects of high linear energy transfer (LET) particle radiation. It is extremely important to study the pathomechanism and the molecular background of previous empirical clinical results and to investigate the biological effectivity of the new beam qualities and to map the innovative binary and multimodal treatment concepts to increase the effectiveness of anticancer therapies.

### ***1. Establishment of optimal parameters of the zebrafish embryo system for radiobiology***

We established an *in vivo*, novel vertebrate model to examine the radiation induced biological effects. The zebrafish (*Danio rerio*) system has several advantages over conventional animal models: simple maintenance, good reproduction rate, large number and small size of transparent embryos, extremely rapid development, external embryogenesis, easy genetic modifiability and the homology between human and zebrafish genome (70%)- all these provide a major advantage for its use in preclinical research, and on the basis of our work proved to be highly applicable in the field of radiotherapy research.

In the course of the research, precise dose delivery techniques, adapted sample holders and the appropriate irradiation geometry of this promising model were determined. Thereafter the biological factors of the zebrafish embryos had been optimized for radiation biology research. To that aim examination of the effects of whole-body single fraction photon irradiation at different dose levels and different ages were performed. We exposed embryos in different post fertilization time points (3 hpf, 6 hpf, 24 hpf) and evaluated several endpoints, such as survival, macro- and micromorphologic alterations in the developing embryos using a light microscope. In our radiation model, the survival, the morphological deteriorations and the histological lesions proved to be age and dose-dependent. The lethal dose (LD<sub>50</sub>) for 6 hours post fertilization (hpf) embryos was 15 Gy and for 24 hpf was 20 Gy on day 7 respectively. The 24 hpf embryos proved to be highly stable, well reproducible and appropriate system for investigations on ionizing radiation effects and on potential radiation modifying agents.

## **2. *Research on radiation modifying agent***

In the first experimental campaign we evaluated a selective radioprotector agent to spare normal tissue during radiotherapy or nuclear accidents. The protective effect of the water-soluble, deacylated phosphorylcholine derivative of L-alpha glycerylphosphorylcholine (GPC) exhibited promising radio-protective effects in our zebrafish embryo model, decreasing the irradiation induced morphological damages and lethality with significant reduction of ionizing radiation caused pro-inflammatory activation. GPC supplementation proved to be a possible future perspective in improving the therapeutic index of clinical radiotherapy treating malignant diseases by selectively protect the healthy tissues in the neighborhood of the target volume.

## **3. *Studies on high LET neutron irradiation, determination of relative biological effectiveness (RBE) of different neutron energies***

Thereafter, being aware that in the earlier life stages embryos are more sensitive to the ionizing radiation, we would have wished to investigate and to compare the biological effectiveness of different radiation qualities using 24 hpf embryos. To that aim, embryos were exposed to reactor fission neutrons, cyclotron based fast neutrons and to conventional photon reference beam (LINAC 6 MV photon). After comparing the survival curves we have found that the biological effectiveness was 10 times higher for high LET thermal neutrons and 2.5 times higher for cyclotron generated fast neutron beam.

Microscopic studies on the embryo morphology *in vivo* and on histopathological slices proved the dose and LET dependent organ malformations (shortening of the body length, spine curvature, microcephaly, micro-ophthalmia, pericardial edema and inhibition of yolk sac resorption) and marked cellular changes in eyes, brain, liver, muscle and the gastrointestinal system.

## **4. *Examination of the biological effects of proton beam at different points of the depth dose curve (plateau, mid of spread-out Bragg Peak (SOBP))***

The increasing use of proton radiotherapy and the rising number of long-term survivors has given rise to a vital discussion on potential effects on normal tissues. The clinically applied generic RBE of 1.1 were only obtained by *in vitro* studies, whereas indications from *in vivo* trials and clinical studies are rare. We therefore set out to characterize the effects of plateau and mid-SOBP proton radiation relative to that induced by clinical MV photon beam reference. Based on embryonic survival data, RBE values of  $1.13 \pm 0.08$  and of  $1.20 \pm 0.04$  were determined four days after irradiations with 20 Gy plateau and SOBP protons relative to 6 MV photon beams. These RBE values were confirmed by

relating the rates of embryos with morphological abnormalities for the respective radiation qualities and doses.

In conclusion, our data demonstrated the applicability of the zebrafish embryo system as a versatile, robust and simple alternative model for *in vivo* characterization of radiobiological effects of ionizing radiation with different LET values in normal tissue.

## 1. INTRODUCTION

Radiation therapy is one of the most common method to disrupt the ability of cancer cells to grow and divide to deprive of their multiplication potential in clinical applications despite having harmful effects on healthy tissues. Ionizing radiation is successfully used in patients with various primary and metastatic tumors (Kalifa and Grill, 2005; Larouche *et al.*, 2007). More than 50% of all cancer patients are subject to radiotherapy during the course of their illness with an estimation that radiotherapy contributes to approximately 60% towards curative treatment (Baskar *et al.*, 2012). Photon beam therapy is frequently used in the locoregional treatment of malignant tumor, it has also detrimental effects, with the aim of damaging the DNA of the cancerous cells and can also induce carcinogenesis in the surrounding healthy tissue of the tumor.

Based on several decades of research on radiation biology, we have learned a lot about the pathomechanism and effects of ionizing radiation, which has led to a significant improvement in effective cancer cell killing and the preservation of normal tissue function resulting of refinement in therapeutic methods. In recent years, there has been a marked development of radiation techniques allowing highly selective dose delivery, that have contributed as well to the improvement of cancer treatment outcome remarkably (Peeters *et al.*, 2010, Allemani *et al.*, 2015).

Advanced photon delivery techniques with enhanced conformity and the rapidly growing installations of superconducting cyclotron/synchrotron-based particle therapy facilities have made hadron therapy available for an increasing number of cancer patients (Specht *et al.*, 2015).

Charged particle therapy leads to an increase in dose precision due to the energy deposition characterized by the Bragg peak (Figure1).

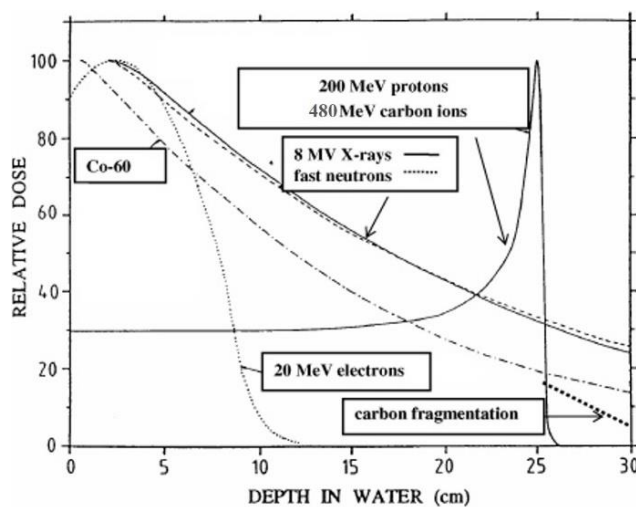


**Figure 1.** Comparison of photon and different particle beams depth-dose curves: fast neutrons,  $\gamma$ -rays, 8 MV X-ray, 200 MeV protons, 20 MeV electrons and 480 MeV carbon ions (Amaldi and Kraft, 2005)

Further innovative radiation approaches are under scientific evaluation including boron neutron capture therapy (BNCT) (Barth *et al.*, 2012), high power laser driven pulsed, ultra-intense, very high energy electron therapy (VHEE) (Schüler *et al.*, 2017), medical microbeam irradiation (Bräuer-Krisch *et al.*, 2015) and Boron Proton Fusion Enhanced Proton therapy (BPFEPT) (Yoon *et al.*, 2014) in order to improve the therapeutic ratio (Hideghéty *et al.*, 2017). During the last years, the more widespread application and the increasing numbers of patients and long-time survivors treated with proton therapy (PT) give rise to discussions on the biological response to proton radiation (Lühr *et al.*, 2018). There is a growing worldwide interest in high-linear energy transfer therapy with new hadron therapy centers and the radiobiology data generated by neutron therapy could help to develop novel *in vivo* model system for investigation of the biological effects and to develop biologically guided treatment approaches. Furthermore, fast neutron experiments are also suitable for the proton RBE simulations in the Bragg peak region, as the majority of the ionization occurs as a result of the formation of recoil protons (Warenius *et al.*, 1994, Jones *et al.*, 2001).

The biological properties of any type of radiation are derived from the energy deposition pattern, which defines the molecular changes, in particular DNA damage and potential repair. It is therefore essential to study the biological effects of the different ionizing radiation qualities and combined approaches to precondition the safe clinical applications.

### ***1.1. Radiation induced damages on normal tissue***

The cellular damage caused by ionizing radiation may vary depending on the cell type, proliferation, intracellular and microenvironmental factors as well as the type of radiation, dose, fractionation and the radiation conditions (Blank *et al.*, 1997, Hendry and West 1997, Olive and Durand, 1997; Meng *et al.*, 1998). Rapidly dividing and immature cells are more sensitive to ionizing radiation than differentiated cells and the target in the cells is DNA (Hall and Giaccia, 2006). The ionizing radiation ionizes the atoms in the tissue it is travelling through, directly interact with cellular DNA and cause damage. The electrons ejected by ionization can either straight act on the target or through the formation of free radicals, mainly from the radiolysis of water, producing subsequently reactive oxygen species (ROS) and reactive nitrogen species (RNS) which can attack cell membranes or break chemical bonds in biological molecules, leading to oxidative stress or DNA damage, termed indirect effect (Baskar *et al.*, 2012, Hurem *et al.*, 2017, Jarvis and Knowles, 2003). Whether the direct or indirect action is dominating, depends mainly on the LET of the radiation, meaning the loss in energy of a charged particle per unit length of path of the medium it is travelling through. Therefore, low LET radiation, such as X- or  $\gamma$ -rays, rather acts by free radicals whereas high LET radiation, like

neutrons or  $\alpha$ -particles, which obviously have a higher biological effectivity, mainly damages the tissue by direct means (Prasad, 1995, Tubiana *et al.*, 1990).

The damage produced by free radicals is furthermore enhanced in the presence of oxygen, by the so called oxygen effect, typical for low LET radiation. This is because oxygen also reacts with free radicals and other molecules in the target tissue to form additional reactive compounds, like hydroperoxy radicals, hydrogen peroxide or organic peroxy radicals, which contribute to the damaging of biological structures. Looking at the whole issue from a cellular perspective, it is to say that the main target of damage, next to RNA, proteins and cell membranes, is DNA, being the most sensitive molecule to ionizing radiation. The most dangerous lesions are double strand breaks (DSB), which in contrast to single strand breaks (SSB), cannot be repaired by resynthesis from the opposite DNA strand, and instead lead to chromosomal mutations. Depending on the nature of the chromosomal change, the mutation might be without consequences, may lead to cell death or induce the formation of cancer if the mutation happens to either turn on an oncogene or turn off a tumor suppressor gene (Hall and Giaccia, 2006, Seymour and Mothersill, 1991).

### ***1.2. Therapeutic index***

The therapeutic ratio indicates the association between the probability of tumor control and the likelihood of normal tissue damage. Improved therapeutic ratio represents a more favorable compromise between tumor control and toxicity (Zindler *et al.*, 2015, Joiner and Van der Kogel, 2009). There are several ways to increase the therapeutic index, the ratio between therapeutic effect and damage of healthy tissue: prolongation of treatment time, hyperfractionation or the use of radio-sensitizers and radio-protectors which specifically increase the sensitivity of tumor cells (Prasanna *et al.*, 2012). Radiation induced damage at the membrane and DNA level can be modified either using sensitizers or protective agents. In the case of cancer therapy, both the selective tumor cell sensitizer and normal tissue radio-protective agent could enhance the efficacy of radiotherapy (i.e. the therapeutic index could be improved).

For every course of radiation therapy, potential benefits should be measured against the risk of normal tissue damage. Since the doses required to achieve tumor control generally overlap with those that may cause complications the normal tissue damage cannot be completely avoided (Beasley *et al.*, 2005). Therefore research on healthy tissue tolerance is of utmost interest. During the radiation therapy the normal tissue protection is essential in order to improve the therapeutic ratio, for that reason, we investigated the effects of a potential radio-protector agent.

### **1.3. Radiation modifiers**

There are expectations and hopes in a wide range of pharmaceutical agents, many of the chemotherapeutics potentiate the desirable effects of radiation therapy. The use of radiation modifying agents allows to test the sensitivity of a biology system to detect differences in radiation effect. Furthermore, there is a great interest in developing radio-protectors to prevent normal tissue toxicity during chemo- and/or radiotherapy or nuclear accidents. Although most of the agents showed to be toxic to normal tissues at therapeutic doses, few compounds already passed their clinical trials and can be successfully applied to improve the therapeutic outcome of some tumors. The selective protection of healthy tissues surrounding the tumor is at least to the same extent important as the treatment of tumor cells to make them more susceptible to radiation damage (Prasad, 1995). There are different possibilities for their mechanism of action like reduction of ionized molecules, decreasing radiation-induced inflammation (Daroczi *et al.*, 2009), DNA repair (Bladen *et al.*, 2007, Hwang *et al.*, 2007) and stabilization of membranes.

#### **1.3.1. Potential therapeutic effects of phosphatidylcholine**

Phosphatidylcholine (PC) is an essential component of endogenous surface-coating substance and biomembranes, and it is well founded that it is key lipid component of all kind of cell membranes and blood proteins (Volinsky and Kinunnen, 2013). PC serves in the central nervous system (CNS) as the main source of choline, an essential nutrient and precursor to the neurotransmitter acetylcholine and has an enhanced role in mucosal cells, which maintains lung function and gastrointestinal health (Treede *et al.*, 2009). GPC is a water-soluble, deacylated PC intermediate which may be hydrolysed to choline and has been developed and studied as a potent anti-inflammatory and neuro-protective agent (Gallazzini and Burg, 2009). Research suggests that GPC positively enhances the inflammatory response and potentially reduces the tissue damage caused by IR (Erős *et al.*, 2009, Gera *et al.*, 2007, Tökés *et al.*, 2014). GPC can be hydrolyzed to choline and possibly used for the resynthesis of PC (Gallazzini and Burg, 2009). Brownawell *et al.* (2011) investigated the toxicity of GPC in rodents by examining the acute, subacute and late effects of different GPC doses from 100 mg/kg bw to 1000 mg/kg bw in rats. The acute lethal dose of intravenously (i.v.) administered GPC was 2000 mg/kg bw and the intraperitoneal (i.p.) dosing of rats produced mortality starting at 1500 mg/kg bw while oral administration resulted in mortality from 10000 mg/kg bw. In subchronic or chronic studies, doses of 100 and 300 mg/kg bw, GPC did not alter the behavior, body weights, haematology or clinical chemistry of rats and did not produce any signs of general toxicity. In haemorrhagic shock experiments, (a prototype of systemic IR), concentrations of GPC significantly lower than the well tolerated dose, caused rats to recovery to baseline levels after 24 hours (Scribner *et al.*, 2010). GPC

has proved effective against the loss of the membrane function in CNS injuries (Amenta *et al.*, 1994, Onishchenko *et al.*, 2008). GPC was previously tested as a centrally acting parasympathomimetic drug in dementia disorders and acute cerebrovascular diseases (Barbagallo *et al.*, 1994, Moreno 2003, Parnetti *et al.*, 2007) and was found to inhibit the transfer process of bifunctional phospholipid transfer protein (Komatsu *et al.*, 2003). GPC, after oral administration, has been shown to cross the blood-brain barrier (BBB) and reach the CNS, where it is incorporated into the phospholipid (PL) fraction of the neuronal plasma membrane and microsomes (Tayebati *et al.*, 2011). Furthermore, GPC has also been proven to protect membranes from oxidation and is able to improve membrane function after traumatic damage (Onishchenko *et al.*, 2008, Kidd, 2009). GPC has been exhibited protective activity in different experimental models against damage occurring due to inflammatory reaction (Tőkés *et al.*, 2015). In a rat focal-brain irradiation model, GPC was proven to alleviate the radiation-induced decline in cognitive function and to decrease the microscopic brain damage (Plangár *et al.*, 2014, Drago *et al.*, 1992). Experiments of Tőkés *et al.* (2011) and Ghyczy *et al.* (2008) have shown PC to be effective in stopping the production of ROS both *in vitro* and *in vivo* and may exhibit anti-inflammatory properties (Onishchenko *et al.*, 2008, Kidd, 2009).

#### **1.4. Different radiation qualities**

##### **1.4.1. Neutron irradiation**

Neutrons are a member of high LET radiation and therefore possess a higher biological effectivity, however, also have the potential to cause more damage in healthy tissues. Not only their energy is higher, neutrons also distribute in a much more precise way in the target tissue, all their energy concentrates on a few paths as compared to  $\gamma$ -rays whose energy is much more spread out. Figure 2 shows this phenomenon, with  $\gamma$ -irradiation on the left side and neutron on the right (Tubiana *et al.*, 1990).

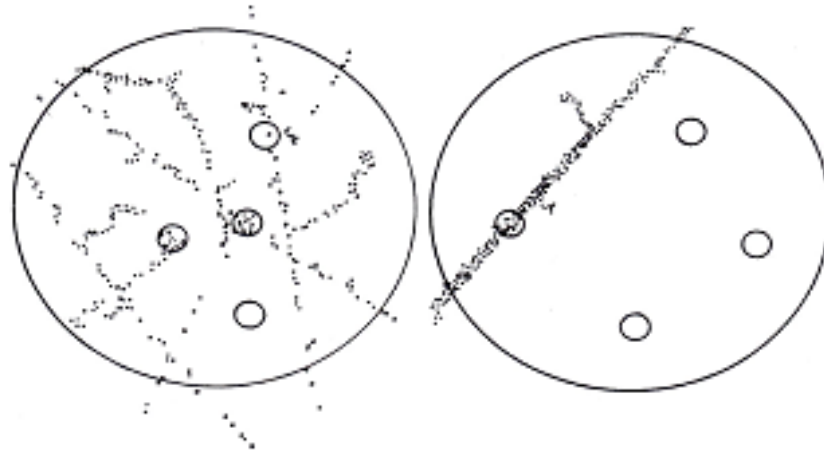


**Figure 2.** Distribution of radiation in the target tissue (Tubiana *et al.*, 1990).

Furthermore, neutrons decrease the oxygen effect, which is very pronounced in the case of X- and  $\gamma$ -radiation, and their effectiveness is much less dependent on radiosensitive phases of the cell cycle than X- or  $\gamma$ -radiation (Seth *et al.*, 2014). These facts may be of an advantage depending on the type of the tumor. Suitable candidates for neutron therapy are therefore patients in whom hypoxia of tumor cells is the cause of radioresistance or in whom conventional therapy is limited because of less tumor cells in the radiosensitive phases of the cell cycle. The tumor should also be superficially seated as the penetration depth of neutron beams is low (Tubiana *et al.*, 1990). High LET, and consequently high RBE, radiation combined with a high selectivity of dose deposition has tremendous advantages over low LET beams for the local control for radio-resistant, hypoxic tumors - even in critical anatomical location. One of the first large clinical scale attempts to use high RBE radiation was fast neutron therapy in the 70s and 80s (Specht *et al.*, 2015). Highly contradictory results were obtained at these first generation neutron facilities and actually only four fast neutron facilities with improved delivery technique (3D planning, conformal/intensity modulated RT) offered fast neutron therapy (FNT) for patients with salivary gland tumors, sarcomas and malignant melanoma (Liao *et al.*, 2014).

#### 1.4.2. Proton irradiation

Proton radiotherapy (PT) is hadrontherapy's fastest growing method and the pillar of the fight against cancer which has rapidly evolved from the pioneering trials at the end of the 20<sup>th</sup> century to become an accepted alternative to conventional external beam radiotherapy (EBRT) with photons. These particles have shown to represent a high impact on the improvement of cancer therapy, mainly because of their preciseness of dose delivery selectively to the cancer (Levin *et al.*, 2005). The beam have a well-describable path, with the release of their energy maximum in a huge spike, the so-called Bragg peak, at its end. Figure 3 visualizes this phenomenon, representing the tissue distribution of entering proton radiation.

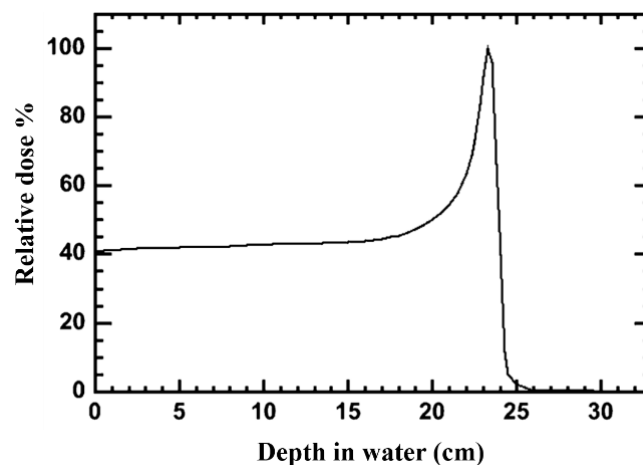


**Figure 3.** Depth-dose distribution for the proton beam (Rosenfeld *et al.*, 2004).

Due to this advantageous property, the tumor volume can be very precisely targeted with higher dose deposition at the end of the proton track, in the Bragg peak, means that PT offers the possibility of sufficient dose delivery to the tumor whilst simultaneously sparing the surrounding normal tissue (Hall and Giaccia, 2006). In recent years, the widespread use and the increasing number of patients treated with PT and long-term survivors give rise to focus research on the biological response along the proton beam absorption path (Lühr *et al.*, 2018). So far, treatment planning and evaluation in PT is based on a fixed generic RBE of 1.1, which describes a 10% higher cell killing efficiency for protons relative to photons as an average over the depth dose curve. The increased LET at the end of the SOBP is correlated to an enhanced RBE which might be of risk for the surrounding normal tissue in particular in the normal tissue distal of the tumor (Paganetti, 2014; Lühr *et al.*, 2018). One of the few clinical studies that provide evidence for such variable RBE was published by Peeler *et al.* (2016) who correlate alterations in magnetic resonance images with RBE variations of clinical proton depth dose curves. The limited available animal data reveals a less pronounced increase than the RBE value of 1.6 found in *in vitro* cell studies (Gueulette *et al.*, 1997; Paganetti, 2014; Saager *et al.*, 2017, 2018; Sørensen *et al.*, 2017). Exemplarily, moderately increased RBE values of  $1.13 \pm 0.04$  for the entrance region and of  $1.26 \pm 0.05$  at the distal end of a 6 cm proton SOBP were found by Saager *et al.* (2018) rating the occurrence of myelopathies after rat spinal cord irradiation and using MV photons as reference. One of the main challenges for such purposive *in vivo* studies on the RBE-LET correlation is the precise and reproducible positioning of animals and target volumes along the proton depth dose distribution. Likewise, in clinical patient treatment, anatomical changes, positioning uncertainties and organ movements might result in deviations from the desired beam position in the body, especially at the distal end of the proton path (i.e. the proton range; Richter *et al.*, 2016).

### ***1.5. Zebrafish as a model system***

Cell cultures and small mammalian animals are well established widely-used models for preclinical investigations. In the era of rapid development of highly selective and combinative radiation technology, there is a need for a new *in vivo* model for studying the effects of different radiation qualities and radiation modifiers in a complex organism (Steel, 1993). In the present work, we choose to validate the zebrafish embryo model an alternative *in vivo* vertebrate system for assessment of the biological effects of ionizing radiation.

Zebrafish (*Danio rerio*) embryos have recently been introduced as a widely used novel vertebrate preclinical research model (Geiger *et al.*, 2006). Their genomes share major homology with the human genome, making them amenable for the study of various human diseases of oncogenic, neurodegenerative, hematopoietic and cardiovascular origin (Zon, 1999, Amatruda *et al.*, 2002,

Daroczi *et al.*, 2006, Hwang *et al.*, 2007). Zebrafish are excellent tools for experimental human cancer research as many key genes involved in cell cycle, oncogenesis, tumor suppression are conserved between the two species (McAleer *et al.*, 2005). This vertebrate model is an ideal test system as they have many positive attributes including good reproduction captivity and easy laboratory care at a relatively low cost. Embryo development is extremely rapid during the first few days post-fertilization whilst the embryos and larvae are transparent, giving the possibility to study the *in vivo* organ development and perturbations (Bailey *et al.*, 2009, Geiger *et al.*, 2006, Hwang *et al.*, 2007). Zebrafish have a full complement of vertebrate-specific organs of radiobiological interest, including brain, eyes, spinal cord, vasculature and digestive, excretory and hematopoietic systems. Furthermore the zebrafish has wide tolerance regarding their maintenance (Daroczi *et al.*, 2006) and transportation. These small Asian fishes can be rapidly bred in large numbers and the embryos does not require sterile conditions, like the cell cultures, and thus are better suited for radiobiological studies at non-hospital research radiation sources. The zebrafish model represents an important step between *in vitro* cell culture experiments and small animal studies. In contrast to cell cultures, the embryos are whole vertebrate organisms, therefore complex biological processes can be investigated, can be used for the abscopal effect (Yasuda *et al.*, 2017) and immunogenic reactions (Langheinrich, 2003) investigations. Zebrafish embryos are permeable to drugs, dyes, small molecules, as well as peptides, and can be transfected to express genes in tissue specific manner.

These features, combined with other properties, including a high genetic similarity of 70% to human, e.g., genes of the DNA repair machinery (Pei and Strauss, 2013), easy handling in experimental conditions and optical transparency that facilitate continuous observation of organ perturbations, favors the zebrafish embryo for radiation research of normal tissue response (Stern and Zon, 2003; Barriuso *et al.*, 2015, Geiger *et al.*, 2008). With an irradiation size of about 1 mm, between cell monolayer culture and subcutaneous tumors or normal tissue organs in small animals (mice, rat), the zebrafish embryo could potentially be deployed for detailed investigations on the RBE-LET correlation and to quantify the low LET and high LET radiation induced damages at the total organism, at organ and at tissue level.

### ***1.6. Biological model development for research on laser driven proton sources***

The installation of ultrafast, high-energy lasers opens the possibility for development of innovative approaches in radiation oncology. There has been a vast development of laser-driven particle acceleration (LDPA) using high power lasers, resulting in short particle pulses of ultrahigh dose rate. At the actual status of the development, low energy, limited size beams are available under technical

conditions for radiobiology experiments, therefore the zebrafish embryo as a small vertebrate model for comparative radiobiology studies can be used for laser driven proton irradiation.

## 2. AIMS

Our aims were to develop and validate an appropriate *in vivo* preclinical model in order to achieve radiobiological effect assessment focused on healthy tissue reactions. The establishment of a zebrafish embryo model for comprehensive radiobiological research stands in the focus of our investigation, comparing the radiation effect curves of neutron, proton and photon sources. We propose integrated radiation setups for reproducible irradiation, system of post radiation detection, histological and molecular investigations on correlations of the changes caused by different radiation sources.

We set out to determine tolerability and possible toxic effects of different radiation modifying agents which can moderate the radiation-induced, functional and morphological changes. Derivate goal was to examine the cytokine response with a potential anti-inflammatory intervention. Our further aim was to develop and validate the small vertebrate preclinical model in order to investigate the relative biological effectiveness of LDPA.

In summary, the aims of our studies were:

- a) establishment of optimal parameters for validation of the zebrafish embryo model, definition of embryonal stages, doses and observational endpoints;
- b) to develop a precise dose delivery technique and setup for reproducible irradiation;
- c) to define the radiation dose-effect curves and to establish the most appropriate dose for research on radiation modifiers;
- d) to examine the effects of the anti-inflammatory agent: L-alpha glycerylphosphorylcholine (GPC);
- e) to define the Relative Biological Effectiveness of divers high LET radiation;
- f) to characterize the effects of plateau and mid-SOBP proton radiation relative to that induced by clinical MV photon beam reference.

### **3. MATERIAL AND METHODS**

#### **3.1. *Animal model***

Laboratory-bred, wild type strain (AB) of zebrafish (*Danio rerio*) were kindly provided by the Department of Aquaculture, Szent István University, Gödöllő. The animals were held in an aquarium system, at the Department of Medical Physics and Informatics, University of Szeged, Faculty of Science and Informatics. The experimental protocol was approved by the Ethical Committee for the Protection of Animals in Scientific Research at the University of Szeged (XXXII./1838.2015) and followed the National Institutes of Health (Bethesda, MD, USA) guidelines on the care and use of laboratory animals.

Adult fish were maintained separated by sex; with favorable conditions of the recirculation water system, an optimal temperature of about 27.5 °C and a regulated 14-hour light/10 hour dark cycle, fed three times a day on a varied diet, commercial dry fish food supplemented with freshly hatched brine shrimp (*Artemia nauplii*) according to standard procedures (Westerfield M, 2000).

#### **3.2. *Embryo harvesting and maintenance***

Wild-type adult fish (2 female and 3 male) were mated in embryo breeding tanks in the afternoon and the eggs were spawned the following morning. Viable embryos were washed with 0.1% methylene blue solution, sorted under a stereomicroscope (Stemi 508, Stand K LAB, Carl Zeiss), transferred to a 10 cm Petri dishes containing 5 ml E3 embryo medium (5 mM NaCl, 0.17 mM KCl, 0.33 mM CaCl<sub>2</sub>, 0.33 mM MgSO<sub>4</sub>, 0.1 % methylene blue) and maintained under normoxic conditions at 27.5 °C.

#### **3.3. *Method of establishment of the zebrafish embryo model for radiobiology***

##### **3.3.1. *Test organism***

Experiments were performed on viable embryos, of 3-, 6-, and 24 hours post fertilization (hpf). Embryos were sorted, 1 embryo/well of standard 96-well polystyrene microplates in 250 µl embryo medium at the one-to two-cell stages, and kept under normoxic conditions at 27.5 °C, according to the standard handling procedure. The embryo medium in each well was changed daily to avoid contamination and spread of infection.

##### **3.3.2. *Irradiation treatment***

Embryos dispensed individually in 96 well plates, were exposed to  $\gamma$ -radiation of doses ranging between 0 Gy and 20 Gy, in 5 Gy increments. There was one control group and five exposure groups, in total, consisting of 96 embryos (n=96) each.

Irradiation was performed by a Teragam K-01 (SKODA UJP, Prague, Czech Republic) cobalt unit with an average energy 1.25 MV, source isocenter distance 80 cm.

For achieving the required build-up effect, the plates were placed between two polymethyl methacrylate (PMMA) slabs of 2 cm thickness. The isocenter was positioned in the plates' geometrical centers. In order to maximize the field homogeneity, half of the planned dose was delivered by a 20 x 20 cm beam downward (gantry angle 0°), while the other half with an identical beam upward (gantry angle 180°). This isocentric setup ensured that the dose uncertainty originating from the movements of the embryos could be eliminated (Figure 4). Irradiation time correction factors were used to compensate for the decay of the Cobalt-60 source. After radiation treatment, the embryos were kept at optimal conditions for a seven days observation period and were examined under a light microscope.

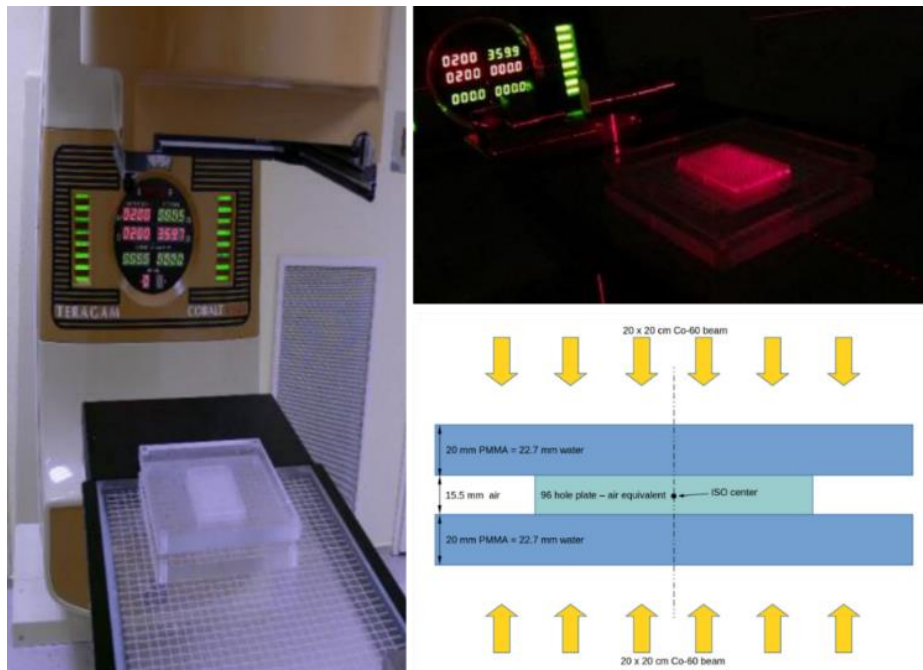


**Figure 4.** The radiation exposure experimental setup.

### 3.3.3. Morphology and survival analysis

In order to establish the age-related dose-response survival curves, and to detect the morphological abnormalities, individual embryos were continually assessed for survival in each experiment in 24-hour intervals from fertilization to 192 hpf. The embryos were observed without any manipulation in the microplates and were incubated at 27.5°C. Viability was analyzed with light transmission using a Nikon Eclipse TS100 inverted microscope (Nikon Americas Inc. Melville, NY) at 10X, 20X magnification and representative images were acquired at 10X magnification using a Nikon Coolpix 4500 (4.0 mega pixels 4X zoom) camera. Dead embryos were removed daily and the number of viable

and malformed embryos were registered. Survival was calculated as a percentage of viable embryos to the total number of embryos exposed in each treatment group over time. The criterion of embryonic survival was the presence of cardiac contractility. Similarly, morphology was assessed visually and photo-documented. The size and shape of the embryo, skull, spine and tail, the development of the different organs (eye, brain, and midline), yolk sac resorption, and pericardial edema were evaluated daily in the proportion of the living embryos.

#### **3.3.4. Histopathology**

For histological assessments, the groups of control and treated embryos were sacrificed after 7 days of observation placed in 1:100 dilution of 4 mg/ml tricaine methanesulfonate (Sigma-Aldrich®) then fixed by immersion (4% paraformaldehyde for 3 days), and embedded in paraffin. Transverse whole-body sections (4  $\mu\text{m}$  thickness) were taken and stained with hematoxylin and eosin (H&E). Sections were analyzed using a Zeiss Axio Imager Z1 light microscope (Zeiss EC Plan Neofluar 5X/0.16, 10X/0.3, 20X/0.5 M27, Germany) at 5X-20X magnification, and photomicrographs were taken using an AxioCam MR5 camera equipment.

### **3.4. Studying the effects of the radiation modifier**

#### **3.4.1. GPC pre-treatment**

Zebrafish embryos at 24 hpf were incubated in GPC (Lipoid GmbH, Ludwigshafen, Germany; 25 mg dissolved in 1 ml single distilled water). A toxicity test was conducted using different dilutions in the absence of radiation. GPC (194.0  $\mu\text{M/L}$ , 243.0  $\mu\text{M/L}$ , 324.0  $\mu\text{M/L}$ , 468.0  $\mu\text{M/L}$ , 972.0  $\mu\text{M/L}$ , 1944  $\mu\text{M/L}$  from 9720  $\mu\text{M/L}$  stock solution) was added to embryos for 3 hours then the medium was changed and embryos were maintained at 27.5°C for 168 hours to define survival and morphological changes.

After the toxicity assessment, the GPC at 194  $\mu\text{M/L}$  dose level was used to examine the radiation modifier effect on healthy tissues. Embryos were divided into four groups: control, GPC-treated, irradiated, GPC-treated followed by irradiation. They were incubated for 3 hours and exposed to 20 Gy at 24 hpf for survival and morphological analysis and to 10 Gy at 24 hpf for molecular examination. The irradiation was performed as described previously, in 96 well plates (1 embryo/well) with Cobalt-60 beam.

#### **3.4.2. Survival and morphology assessments**

To quantify the toxic and radiation modifier effects of GPC on survival, growth and morphological disorders, daily microscopic examination was performed. The procedure was implemented as described above, the survived and distorted individuals were recorded and evaluated.

### **3.4.3. Quantitative Polymerase Chain Reaction (qPCR)**

After 1 and 2 hour post treatment, the inflammatory cytokine level was measured. To ensure adequate biological material for the measurement, three replicates were generated from each experimental group by pooling 20 embryos in 2 ml homogenization tubes.

The total RNA was isolated in Trizol (Invitrogen, Carlsbad, USA). Tissues were homogenized using a homogenizer (IKA, T10 digital ULTRA-TURRAX) and then chloroform (200  $\mu$ l) was added to the homogenized embryo tissue. RNA was precipitated by adding isopropanol (500  $\mu$ l, Sigma-Aldrich) then the tubes were rotated gently to ensure mixing and incubated for 10 min at room temperature. After centrifugation (12,000 g, 20 min, 4°C) the supernatant was removed and washed in 1 ml 75% ethanol (Reanal, Hungary). The remaining material was dissolved in 22  $\mu$ l RNase-free water. RNA concentration was measured by MaestroNano spectrophotometer. cDNA was synthesized from 1  $\mu$ g total RNA with random hexamer primers using RevertAid First Stand cDNA Synthesis Kit (Thermo Scientific, USA) according to the manufacturer's instructions. Real-Time PCR were performed using an CFX 96 Real Time System (Bio-Rad, USA) to detect changes in mRNA expression, using 4  $\mu$ l of diluted cDNA template mixed with 1 $\mu$ l of each primer and 10  $\mu$ l of SYBR Green PCR Master mix (Applied Biosystem, USA) at a final volume of 20  $\mu$ l with a thermal cycle (95 °C 2 min) followed by 40 amplification cycles (95 °C 10 s then 60 °C 30 s).

IL-1 $\beta$  and NF- $\kappa$ B levels were measured using sequence-specific TaqMan gene expression assays (Life Technologies) with 18S rRNA used a pre-optimized primer and probe assay (Applied Biosystem, USA) for endogenous control. Each PCR reaction was repeated and the relative mRNA level was calculated by the  $2^{-\Delta\Delta CT}$  method (Livak and Schmittgen, 2001).

### **3.4.4. Histopathology**

Histopathological procedures were the same as described above. Sections were analyzed under an Axio Imager Z1 (Zeiss EC Plan Neofluar 5X/0.16, 10X/0.3, 20X/0.5 M27, Freiburg, Germany) light microscope, and photomicrographs were taken with AxioCam MR5 camera equipment. At least 15 embryos from each treatment group were observed by two independent investigators.

## **3.5. Method of RBE definition of different high LET sources**

### **3.5.1. Embryos handling**

Fertilized embryos in the pharyngula period (24 hpf) were individually placed in wells of a 96-well plate, with 250  $\mu$ l embryo medium, for conventional photon irradiation. For comparison of different radiation qualities found in different institutions, embryos at the same stage of development were used, but regarding the neutron facilities the embryos were floating in E3 medium in eppendorf tubes for

the irradiation period. After the radiation treatments the embryos were transferred to plates and final assessment was performed at 168 hours post irradiation. The experiments were repeated three times with 96 embryos (n=96) in each experimental group, at all visited centers. The local Animal Ethics Committee had approved all experiments. To ensure the standard 27.5°C required optimum temperature, a portable incubator (Ranger MX45, Lynd Products) was used.

### **3.5.2. Photon irradiation**

6 MV photons, generated by a linear accelerator (Primus2 Siemens, Department of Oncotherapy, University of Szeged), was used as a reference beam. The plates were positioned between two 2 cm PMMA slabs to assure a homogeneous radiation exposure. The isocenter was positioned in the plates' geometrical centers. Groups were treated at room temperature with 0 Gy, 5 Gy, 10 Gy, 15 Gy, 20 Gy doses with a dose rate of 3 Gy/min and a source to surface distance (SSD) of 100 cm. The required doses were delivered in two portions with half of the dose delivered upwards and the remaining downwards by means of a rotating gentry (Figure 4).

### **3.5.3. Fission neutron irradiation**

Neutron irradiations were performed at the Budapest University of Technology and Economics, using the Training Reactor "pneumatic rabbit" system. The outer diameter of the pneumatic polyethylene tube system was 25 mm, the wall thickness was 2 mm and the inner diameter was 21 mm. The sample irradiation capsule, also made of polyethylene with a maximum sample mass of 30 g, was in the center of the tube. The capsule was 50 mm in length and the diameter of the capsule was 14 mm. Irradiation time were possible from 2 seconds up to 2 hours and the delivery time was 3 seconds. The pneumatic rabbit system has two types of connections: The "quick" channel in the core of the reactor and the "thermal" channel, in the water (Figure 5). All zebrafish embryo irradiation was carried out in the thermal channel at dose levels: sham irradiated, 1.25 Gy, 1.875 Gy, 2 Gy, and 2.5 Gy. The power of the reactor during the experiment was 200 W and the irradiations lasted 36, 49, 63 and 72 s.

The dose rate at the location of irradiation was calculated with the aid of the Monte Carlo transport code MCNP. Detailed 3-dimensional models of the entire core of the training reactor were set up, which were later used, among others, for coupled neutron-photon calculations in order to determine the dose rate. The Monte Carlo model has been validated using neutron flux and dose rate measurements in and near the reactor core.

According to the calculations, the dose rate of the neutrons and photons (gamma-radiation) at the place of the irradiation is  $1.27 \pm 0.04$  Gy/min. Accordingly, doses delivered during the experiments

were approximately between 0.76 and 1.52 Gy for the 36 s and 72 s long irradiations, respectively. The standard deviation of the calculated dose rate only refers to the Monte Carlo uncertainty and does not include modeling and cross section based uncertainties. It was based on literature and previous experience of the authors and the real uncertainty was estimated at 0.14 Gy/min.

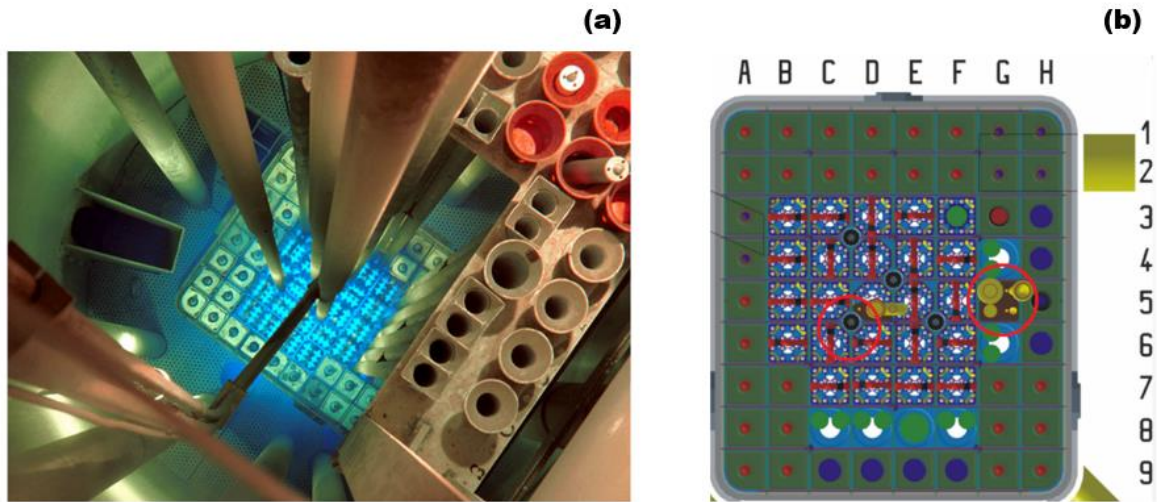


**Figure 5.** The Training Reactor of the Budapest University of Technology and Economics. (a) Training Reactor core as seen from above during 100 kW power operation. (b) Layout of the reactor core and the “pneumatic rabbit” system (red circles).

#### 3.5.4. Cyclotron generated fast neutron radiation

Three irradiation experiments were performed at Hungarian Academy of Sciences, Institute for Nuclear Research - Atomki Institution, with cyclotron generated neutrons. The zebrafish embryos were exposed to the mixed neutron-gamma field of the p(18 MeV)+Be fast neutron irradiation facility (Fenyvesi, 2004) based on the MGC-20E cyclotron, at 0 Gy, 2 Gy, 4 Gy, 6.8 Gy, 8.12 Gy and 10.28 Gy dose levels. During each experiment,  $E_p = 18 \text{ MeV} \pm 0.3\% \text{ MeV}$  energy proton beams were transported to the irradiation facility. The beam currents were in the  $I_p = (9.2 - 10.7) \mu\text{A}$  range and they were kept constant during irradiation. The protons passed first a stainless steel entrance window foil and then a layer of flowing helium gas that cooled the bombarded target surface. The average energy loss of the protons was  $\langle \Delta E_p \rangle = 0.355 \text{ MeV}$  before reaching the beryllium target that fully stopped the beam. The proton-induced nuclear reactions on  ${}^9\text{Be}$  target nuclei lead to emission of neutrons and gamma photons with continuous broad energy spectra that covered the  $E = 0 - 20 \text{ MeV}$  energy range. Most neutrons were emitted in the  $E_n > 0.1 \text{ MeV}$  energy range and the average neutron energy was  $\langle E_n \rangle = 3.5 \text{ MeV}$ .

The irradiation field was monitored by a twin ionization chamber technique (Broerse *et al.*, 2014) using thimble type EXRADIN T2 and M2 chambers with 3 mm thick build up caps.

The  $D_n$  neutron and  $D_\gamma$  gamma doses and the  $D_{tot} = D_n + D_\gamma$  total doses were calculated for water. The ratio of the neutron and gamma doses for the irradiated samples depended on the irradiation conditions and on the position and environment of the samples (beam focusing, irradiation arrangement, neutron- and gamma-scattering, etc.).  $D_\gamma/(D_n+D_\gamma) = (14 \pm 3)\%$  ratios were obtained depending on the sample. The total dose rate was  $dD_{tot}/dt = (2.2 - 2.8) \cdot 10^{-3}$  Gy/s depending on the irradiation run and the position of the sample in the irradiation arrangement (Figure 6).

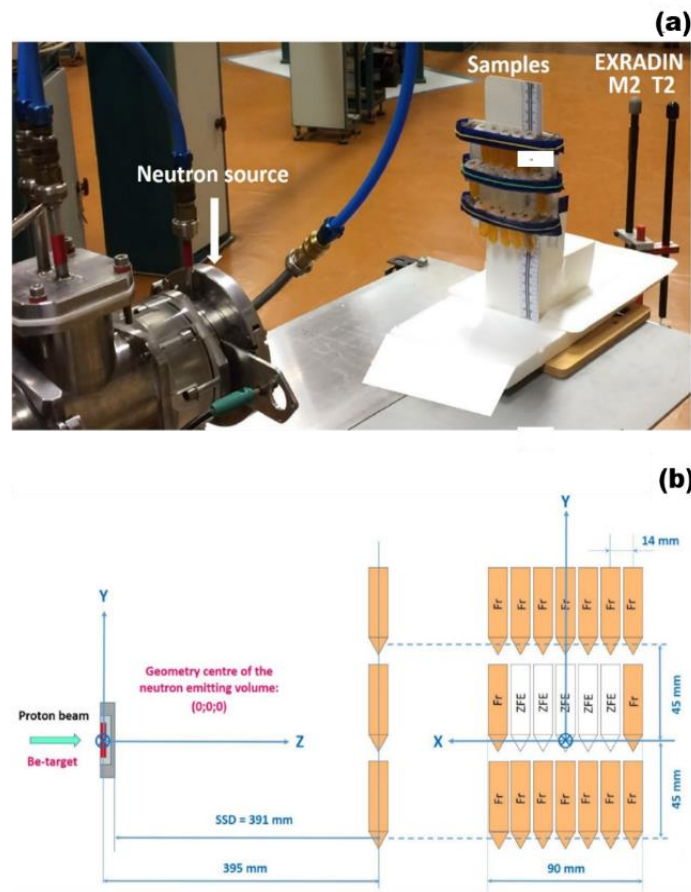


**Figure 6.** The irradiation arrangement at the  $p(18 \text{ MeV})+\text{Be}$  neutron source. (a) The samples and the absorbed dose monitoring twin ionization chambers (EXRADIN T2 and M2) at the  $p(18 \text{ MeV})+\text{Be}$  neutron source of Atomki. (b) The irradiation positions of the zebrafish embryos (ZFE) and the chemical dosimeter solutions (Fr) are shown in the sketch of the arrangement.

### 3.5.5. Analysis of neutron treatment effects on morphology and survival

The developmental status of the embryos, the viability and morphology after irradiation were continually assessed in 24 hour intervals up to 7 days using a light transmission inverted microscope

(Zeiss Axio Imager Z1) and from the deformed specimens photomicrographs were taken. Regular observations were executed in 96 well plates, therefore immediately after irradiation treatments with neutron sources, the embryos from the eppendorf tubes were placed into plates for the observation period. Severe morphological disorders, like pericardial edema, micro-ophthalmia and spine curvature were recorded and evaluated as biological endpoints for the RBE definition (Figure 7). Similar observations were made for the reference photon irradiation. The observation period was executed without any manipulation apart from the addition of fresh embryo medium into the wells on every alternate day, and the embryos were cultured at  $27 \pm 1$  °C with 14-h light/10-h dark cycle during this period. The criterion for embryonic survival was the presence of cardiac contractions. The survival and the morphological abnormalities were evaluated using a total of 4.608 embryos in the proportion of the living individuals as follows:

$$\text{Survival rate \%} = \frac{\text{the number of survived embryos}}{\text{the total number of embryos}} \times 100 \%$$

$$\text{Malformation rate \%} = \frac{\text{the number of malformed embryos}}{\text{the total number of survived embryos}} \times 100 \%$$

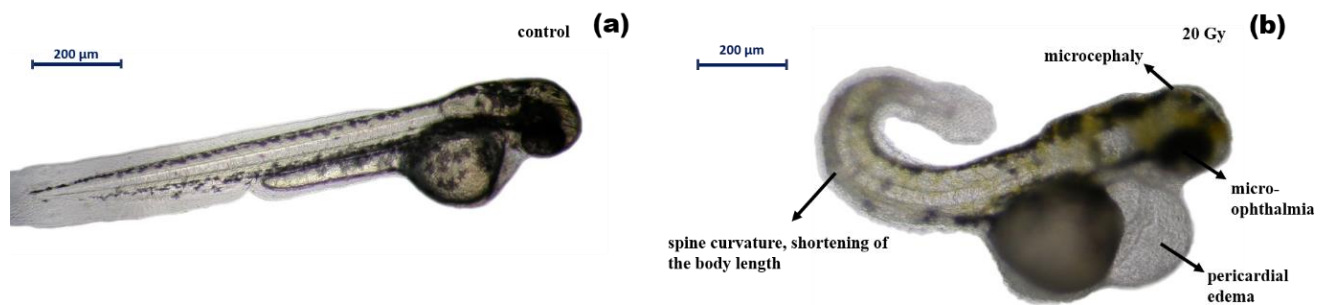


**Figure 7.** Radiation- induced morphologic abnormalities began to appear at 2-3 days post-irradiation in embryos;(a) picture demonstrate a control sample; (b) picture shows the observed abnormalities after 20 Gy.

### 3.5.6. Histopathology and tissue morphology evaluation

Histological examinations were performed on the last day of every experiment, 7 days after irradiation. Samples were prepared for histological examinations as described previously. Sections of 4 µm thickness of sections were stained with hematoxylin eosin (H&E), mounted on glass slides. All sections were analyzed by a Nikon Eclipse TS100 microscope (Nikon Americas, Inc.) at 10x, 20x magnification and scanned with Panoramic MIDI digital slide scanner (3D-HISTECH Ltd., Budapest). Representative images were analyzed for evaluation and recorded using the Panoramic

Viewer 1.14.50 RTM 3DHISTECH from each treatment group at least 15 embryos were observed with the program.

### **3.6. Method for studying the biological effects of the charged particle beam**

#### **3.6.1. Zebrafish embryo handling and preparation**

Zebrafish embryos were kindly provided by the Center for Regenerative Therapies at Technische Universität Dresden (CRTD). Wild type embryos at 24 hpf, i.e. the pharyngula period (24 – 48 hpf), were chosen as for easily ascertainable by the pigmentation of the retina (Gould, 1977). Embryos were washed and sorted into E3 medium, afterwards transported for irradiation at 21 – 22 hpf period with care of the necessary temperature maintenance (28 °C). The embryos were maintained at different temperatures to slow normal embryogenesis (Kimmel *et al.*, 1995) in order to ensure the synchronization of developmental stages of the collected embryos and to compensate for different irradiation time points at the two clinical accelerators, (morning for protons, evening for photons). The developmental stage of the embryos was checked before irradiation by microscopic observation (Axiovert S100, Zeiss, Jena, Germany) and after irradiation the embryos were maintained at 28 °C. During irradiation two embryos in 200 µl E3 medium were placed in the inner 48 wells of 96 well plates (Corning via Sigma-Aldrich Chemie GmbH, Munich, Germany) with the upper and lower row and the two outer columns blank (Figure 8(b)). Because of the horizontal beam delivery the plates were positioned upright and the medium leakage was prevented by stamps that match the reverse profile of the inner 48 wells (Figure 8(b)). The experimental protocol was implemented according to the European Parliament and Council (EU Directive 2010/63/EU). All procedures were performed with respect to this directive and in accordance with German legislation on the care and use of laboratory animals.

#### **3.6.2. Setup for reproducible irradiation at horizontal beams**

For precise positioning and reproducible irradiation of embryos in 96 well plates, a water filled phantom was used (Figure 8(c)(d)) (Beyreuther *et al.*, 2018). The phantom had PMMA walls surrounding the water volume. At beam entrance side the PMMA wall had a defined thickness of  $12.00 \pm 0.05$  mm and the samples can be positioned along the beam axis by moving their holders along four polyvinylchloride bars in parallel to the beam axis. The position of the holder and samples are fixed by PMMA cylinders of appropriate size, which results in a depth positioning accuracy of  $\pm 0.2$  mm. The PMMA cylinders and the usage of multiple holders allows the reproducible and fast positioning of samples at different depths.

For irradiation, the 96 well plates were transported enclosed with their normal lids, which were replaced by stamps directly before irradiation, afterwards the enclosed plates were inserted in the holder (Figure 8(b)(d)).

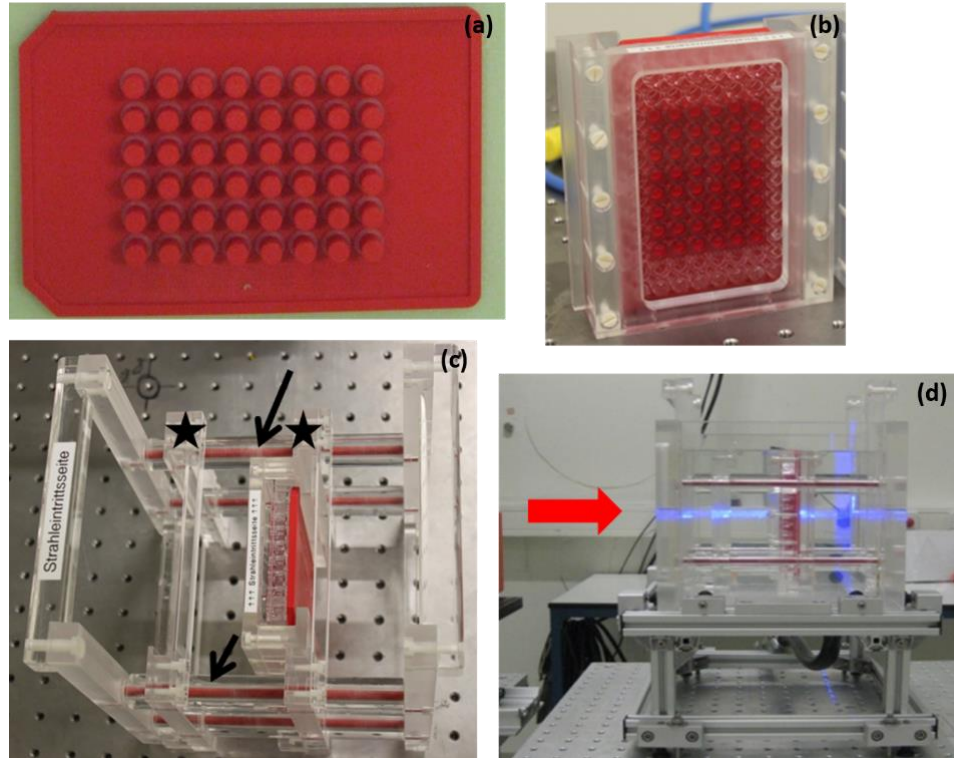


**Figure 8.** (a) ABS stamp and (b) one 96 well plate covered by a stamp plate with the inner 48 wells filled with embryo medium; (c) water phantom insert with holder at mid-SOBP position (\*2). The second, empty holder is fixed by PMMA spacers (arrow) at entrance plateau (\*1) position; (d) complete water filled phantom at the horizontal proton beam (coming from left and marked by the horizontal laser line in light blue) with holder (dark blue).

### 3.6.3. Irradiation with protons

Fixed horizontal monoenergetic pencil-like proton beams in the energy range of 70 - 230 MeV was used at the experimental hall of the University Proton Therapy Dresden (UPTD). Embryos were irradiated with protons at the entrance plateau and in mid-SOBP. For 150 MeV protons a beam shaping system consisting of a double-scattering device and a ridge filter provides a laterally extended proton field of 10 x 10 cm<sup>2</sup> size and a SOBP of variable widths between 20 - 32 mm in water (Helmbrecht *et al.*, 2016). SOBP with a modulation width of 26.33 mm (90% dose plateau) was applied ranging from 86.0 mm to 112.30 mm depth in water. The dose homogeneity is comparable to that achieved for patient treatment with relative dose variations of less than  $\pm 2\%$  over the extended proton field. At both positions of the proton depth dose curve, the verification of the lateral dose

homogeneity was included by the daily quality assurance. Therefore, the phantom is removed and the 2D dose distribution of the unaffected irradiation field is depicted with a Lynx scintillation detector (IBA Dosimetry GmbH, Schwarzenbruck, Germany) revealing potential influences on the irradiation field arising from positional changes of the beam shaping system. The depth dose of the entrance plateau and mid-SOBP was adjusted by one and eleven 7.7 mm thick polycarbonate (PC) plates (water equivalent path length = 1.15 times PC thickness) in front of the Lynx detector.

The dose homogeneity was proven by GafChromic EBT3 dosimetry films (ISP Corp., New York, USA) that were placed directly behind the 96 well plate. After irradiation exposure, the films were air dried, scanned at least two days after irradiation with an Epson Perfection Flatbed Scanner (Epson, Meerbusch, Germany) and analyzed by IDL (Interactive Data Language, Harris Geospatial Solutions, Exelis Visual Information Solutions GmbH, Germany) based software (Zeil *et al.*, 2009). By the result of dose distribution the lateral field inhomogeneity proved to be less than  $\pm 3\%$ .

The sample positioning at the two positions along the proton dose depth curve, at entrance and mid-SOBP within the phantom was checked by a capped Markus ionization chamber (IC) (model 23343, PTW; 1.06 mm water equivalent thickness of entrance window), and the relative depth dose distribution and sample positioning was confirmed by means of EBT3 film stack. Therefore the Markus IC was placed into a special holder (Figure 8) that can be inserted into the holder for the 96 well plates and assures equal positioning of measuring volume and sample.

The dose delivery at the experimental proton beam line was monitored by a beam transmission ionization chamber (IC; model 34058, PTW, Freiburg, Germany) at beam exit that switches off the beam after reaching the requested number of monitor units (MU).

Correlations between absolute dose and radiated MU to water at sample positions at entrance plateau and mid-SOBP within the phantom were determined a daily basis by measurements with a Markus IC at sample position. The different dose depositions at the two sample depth positions were compensated by a higher beam current for irradiation in the plateau region in order to achieve a constant dose rate of 5 Gy/min. Considering the uncertainties of temperature and air pressure during dose measurement, IC calibration and beam quality correction factor a maximum uncertainty of 4.7% was estimated for the absolute dose to water delivered to the zebrafish embryos.

#### ***3.6.4. Photon reference irradiation***

For photon reference irradiations a clinical linac type Artiste (Siemens AG, Erlangen, Germany) at UPTD was used, the gantry was rotated for horizontal delivery of 6 MV photon beams comparable to the proton irradiation. Similar to the proton treatment, the embryos in 96 well plates were positioned and exposed in mid-SOBP position. For radiobiological experiments at the linac the necessary

dosimetry could be related to clinical standard dosimetry with an IC10 (Wellhöfer/IBA Dosimetry) in a homogeneous water filled BluePhantom® (IBA Dosimetry).

The absolute dose to water at sample position and the radiated MU were determined based on clinical standard dosimetry, i.e. correcting the relation of 100 MU = 1 Gy for deviations from standard reference field conditions by using clinical output factors. At sample position the absolute dose was measured with a semiflex IC (model 31010, PTW), where a dose rate of 2.86 Gy/min was achieved. The maximum dose uncertainty was estimated by 3.7% including the suspense from the deviation of air temperature and pressure during dose measurement, uncertainty of clinical daily dosimetry, as well as the depth position uncertainty of the embryos within the sample wells. EBT3 films were positioned behind the sample holder which confirmed that the dose homogeneity was better than 97% over the irradiated area.

### ***3.6.5. Survival and morphology analysis***

Immediately after irradiation the viability of the embryos was assessed using an inverted microscope (Axiovert S100, Zeiss, Jena, Germany). Afterwards, the embryos were separated in one embryo per well and maintained under normal conditions and the embryo medium was changed in every second day. The developmental status of the embryos, hatching rate, survival and morphological abnormalities, such as spine curvature, were monitored daily to the end of the observation time with a Zeiss Observer Z1 microscope (magnification 50x). On the 3<sup>rd</sup> and 4<sup>th</sup> day of observation pictures of the surviving and malformed embryos were recorded using an AxioCam MRm at a Zeiss Axiovert 40 CFL microscope.

The embryonic survival was defined through the assessment of heartbeat and blood circulation.

### ***3.6.6. Scoring system for quantitative analysis of embryo malformations***

In order to categorize the pericardial edema and spinal curvature, a morphological scoring system was adapted (Brannen *et al.*, 2010). Pictures recorded from the malformed embryos on the 3<sup>rd</sup> and 4<sup>th</sup> day post irradiation (dpi) were retrospectively assessed and the malformations were categorized in accordance to the scoring system. In the numerical scoring system for the pericardial edema, score of 1 represented the normal healthy state of the embryos (Figure 9(a)), score 2 meant a variation within the normal range with a very small edema (b), score 3 a marked abnormality where the pericardial edema size was smaller than the head size (c) and score 4 a major disorder with the size of the heart edema equal or even larger than the size of the head (d). For the spinal curvature score of 1 represented normal spine (a), score of 2 a curved end of tail (e), score of 3 a slight bending from half of the body (f), and score of 4 the most severe curvature (g). The mean scoring values ( $SV_{Mean}$ ) describing the

average damage induced by one radiation quality were calculated on the basis of the scored malformations on the 3<sup>rd</sup> and 4<sup>th</sup> dpi, where N represents the number of embryos scored for the respective category.

$$SV_{Mean} = \frac{(4*N_{score\ 4} + 3*N_{score\ 3} + 2*N_{score\ 2} + N_{score\ 1})}{N_{living\ embryos}}$$

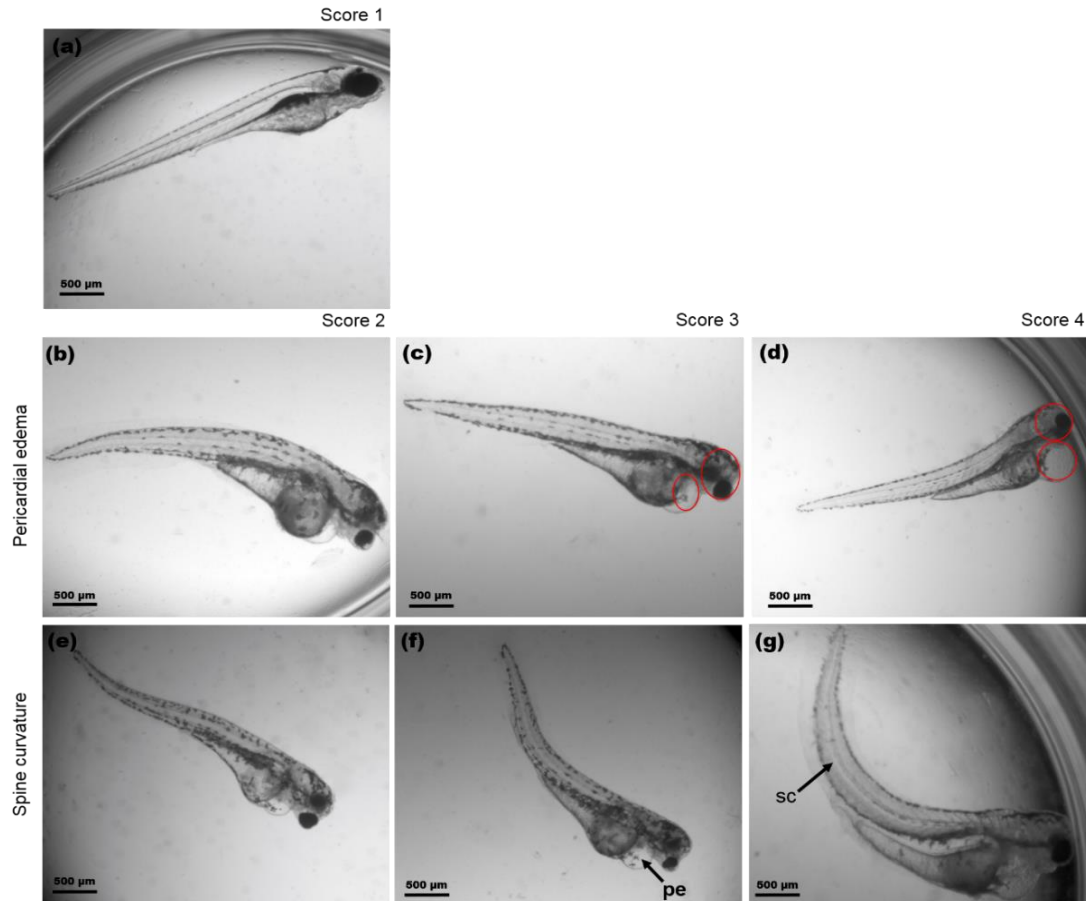


**Figure 9.** Scoring system for the developmental malformation evaluation after irradiation. (a) Normally developed zebrafish embryo, (b-d) scoring for the induced pericardial edema and (e-g) spine bending with increasing severity.

### 3.6.7. Statistical analysis

For age related dose-response survival curves evaluation Kaplan-Meier analyses were performed. The averages of two groups were compared with one-way analysis of variance (ANOVA).

Data assessment of the GPC radio-protection effects were performed using the Cox regression in R statistical programme language (R 3.2.2 for Windows). Statistical significance was defined at  $p < 0.05$ , and data were plotted as means (+standard error of the mean (SEM)) in the graphs.

Measurement of the level of inflammatory cytokine was performed in a commercial statistical software package SigmaStat (for Windows, Jandel Scientific, Erkrath, Germany). Non-parametric methods were used and the differences between groups were subjected to Kruskal-Wallis one-way analysis of variance on ranks, followed by Dunn's method for pairwise multiple comparison. Median values (M) and 75<sup>th</sup> percentiles (p75) and 25<sup>th</sup> percentiles (p25) were plotted and were considered statistically significant if  $p < 0.05$ .

For statistical evaluation of the data for the comparison of survival and the distortion curves of different radiation qualities Log-rank test with Bonferroni correction as well as Chi-square test were applied with GraphPad Prism Version 7.03 Windows. These data were expressed as mean  $\pm$  standard deviation (SD). Levels of statistical significance were taken as  $p < 0.05$ .

For graphical representation of the average survival and the malformation rates of the proton irradiation, were determined a mean value of the three experiment replications, depending on the dose by the Origin Lab 2017 software (OriginLab Corporation, Northampton MA 01060, USA). Groups were compared by using the Log-Rank test with Bonferroni correction (GraphPad Prism Verion 7.04; GraphPad Software, La Jolla, USA) and were considered statistically significant if  $p < 0.05$ . The RBE values were calculated on basis of the average survival for the individual proton dose groups relative to the photon result. The malformation rates at corresponding dose levels for proton and photon treatment were compared by using t-test applying a significance level of  $p < 0.05$ . RBE values were calculated by relating the average of distortion (pericardial edema or spinal curvature) rates obtained for certain proton and photon dose groups and the uncertainties were derived by Gaussian error propagation on basis of the standard deviations of the average malformation rates.

## 4. RESULTS

### 4.1. *Age related radiation dose-response relationship*

Daily assessment of embryo viability during seven days after irradiation showed a strong inverse correlation with the radiation dose. In case of 6 hpf irradiated embryos no relevant mortality occurred at 5 Gy dose level, whilst more than 80% was already dead at 96 hpf at 20 Gy. From day 4, a significant declination of the survival curve was seen at 10 and 15 Gy. At day 7, half of the irradiated embryos were alive, therefore 15 Gy was established as the LD<sub>50</sub> for embryos irradiated at 6 hpf. 100% mortality occurred with 20 Gy irradiation at 6 hpf by day 5 and most died with severe morphologic abnormalities (Figure 10(a)). Lower doses (5-15 Gy) of irradiation caused no relevant mortality up to day 6, for the next day 2-7% of the embryos irradiated < 20 Gy died (Figure 10(c)). Embryos at 24 hpf were less susceptible to radiation, at day 7 the LD<sub>50</sub> was shown to be 20 Gy.

The number of incidence of serious embryonic developmental defects was proportional to the radiation dose and age of the embryos similarly to survival, major distortions occurred earlier if irradiation was performed at 6 hpf. Various distortions were detected after delivery of a dose higher than 5 Gy including a reduction in the body length, spine curvature, microcephaly, micro-ophthalmia, micrognathia, pericardial edema and the inhibition of yolk sac resorption. More than half of the embryos (60-80%) which had received 15-20 Gy showed relevant developmental impairment on the 3<sup>rd</sup> observation day (Figure 10(b)). In contrast, at least 80% of the embryos irradiated at 24 hpf had developed normally, but relevant deterioration occurred during day 4 and increased thereafter at 15-20 Gy (Figure 10(d)).

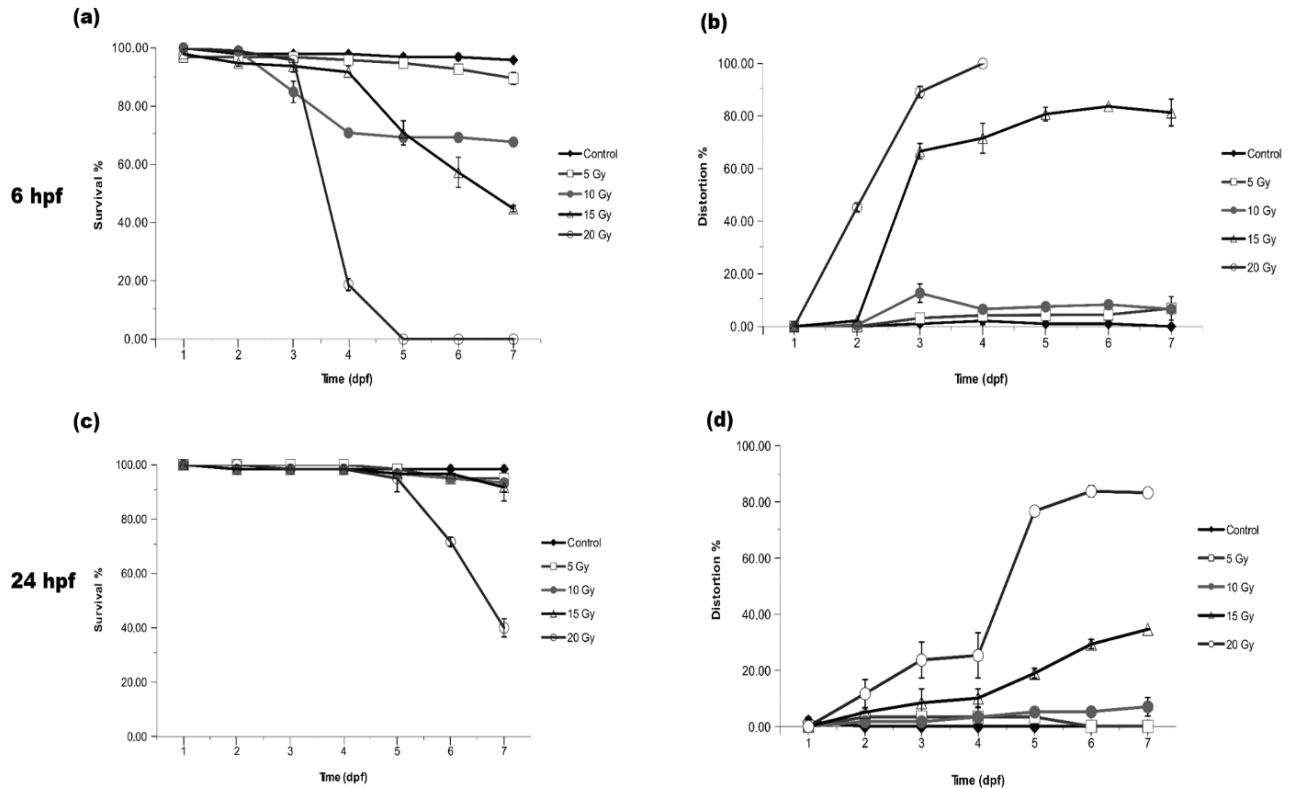


**Figure 10.** The effects of ionizing radiation on zebrafish development and survival. The embryos at 6 or 24 hour post fertilization (hpf) were exposed to 0, 5, 10, 15, or 20 Gy. (a) and (c), the proportion of viable to total zebrafish embryos at 6, 24 hpf. 0 Gy (Control, ◆), 5 Gy (□), 10 Gy (●), 15 Gy (Δ), 20 Gy (○) and survival was determined at 0, 24, 48, 72, 96, 120, 144, and 168 hpf. Morphology was also daily evaluated in each group (b), (d).

#### 4.1.1. Histopathology

The H&E-stained slides showed changes in the skin, such as the disappearance of mucous cells and development of subcutaneous edema in the groups irradiated with 10 Gy at 6 hpf or 20 Gy at 24 hpf, the most severe deteriorations occurred at higher dose levels.

In the observed individuals, the nervous tissue was normal but there were noticeable alterations in the ceratobranchials. There was decrease in goblet cell numbers (Figure 11(a)). In relation to the hepatopancreatic interstitial edema, hydropic and simple pathologic signs of hepatocytes were seen in individuals irradiated at 10 Gy dose level at 6 hpf (Figure 11(b)). Pycnotic changes in the nuclei of the hepatocytes were also observed in the group irradiated with 20 Gy at 24 hpf (Figure 11(c)). Dose dependent pericardial deterioration, such as slight hydropericardium (Figure 11(d)) were observed and this abnormality was more pronounced with increasing doses (Figure 11(e)(f)). In the course of

microscopic monitoring, the stock of vitellin was characterized by vacuoles for the group exposed to 5 Gy at 6 hpf (Figure 11(a)).

Large amounts of mucous and catarrhal were present in the intestinal flux in each irradiated group and goblet cells were found in the intestinal mucous membrane in the group irradiated with 20 Gy (Figure 11(c)). Cells with irregular shapes and with a larger, hyperchromatic nuclei were observed in the 20 Gy irradiated groups.

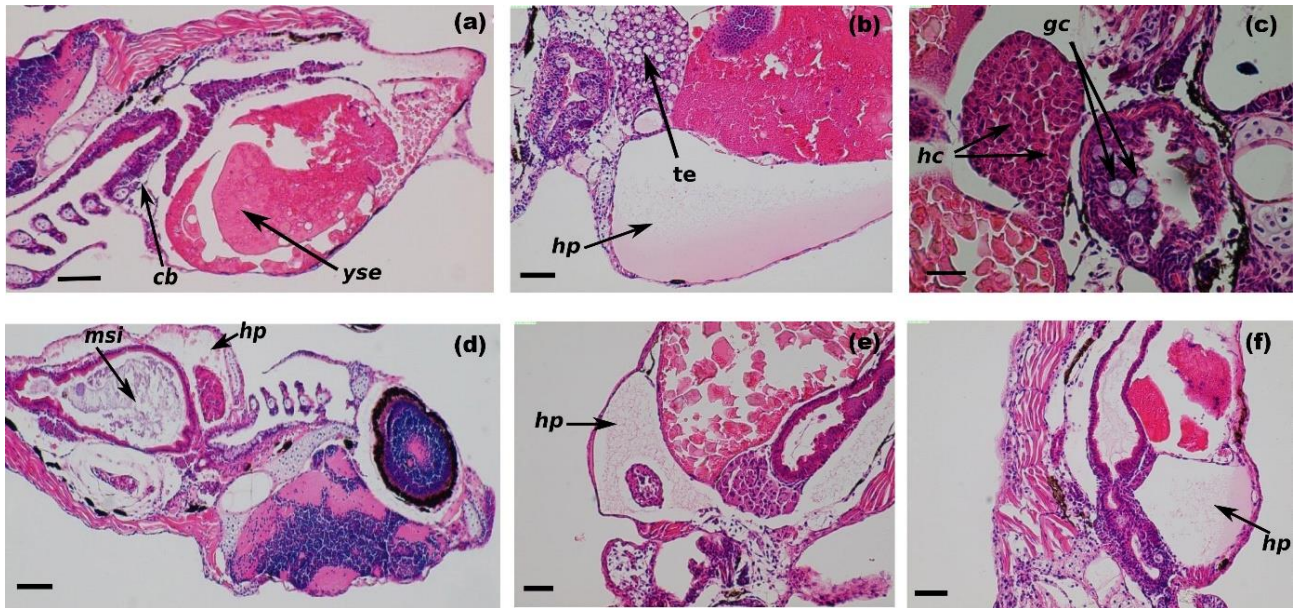


**Figure 11.** The different histological changes in irradiated zebrafish embryos. In (a) there is an observed reduction in the number of goblet cells in the multilayer epithelium of ceratobranchials (cb). Yolk sac edema (yse). Strength of vitellin was characterized by vacuoles. (b) oppressive hydropericardium (hp), tissue edema (te), hydropic and simple pathologic signs of hepatocytes. (c) hepatocytes (hc) with pycnotic nuclei, mucous and several goblet cells (gc) were observed in the gastrointestinal mucous membrane in the intestinal lumen. The degree of hydropericardial disturbances and changes in small intestine. (d) has large amounts of mucous in the small intestinal lumen (msi). Stand by this disorder slight degree of hydropericardium (hp) developed in. (e) severe, serous-fibrinous hydropericardium (hp). Reduction of goblet cells. (f) has severe hydropericardium (hp). Large amounts of mucus were noticeable in the intestinal lumen (HE. 90X. Scale bar 200  $\mu$ m).

#### 4.2. The effects of GPC on survival and distortion

Embryo viability and morphology were not affected by the treatment with escalated doses of GPC using 3 hours incubation time.

Pronounced protective effects were detected at each GPC dose level from 194  $\mu\text{M/L}$  to 972  $\mu\text{M/L}$  administered before IR treatment but there were no perceptible differences between these concentrations. The control and GPC-treated groups were viable at day 7 post treatment. Embryos irradiated with 20 Gy without GPC pre-treatment started to die at day 3, in contrast, all embryos exposed to 20 Gy and treated with GPC were still alive. Survival decreased in both irradiated groups from day 4, but the mortality was more pronounced in the group without GPC pre-treatment. On the 7<sup>th</sup> day, the difference in survival between the GPC pretreated and irradiated group and the irradiated control group was 20%, there were significant differences in survival as well as in the morphologic alterations compared with the control samples. GPC in 194  $\mu\text{M/L}$  concentration with 3 hours incubation prior to the radiation delivery had significant protective effects (Figure 12).

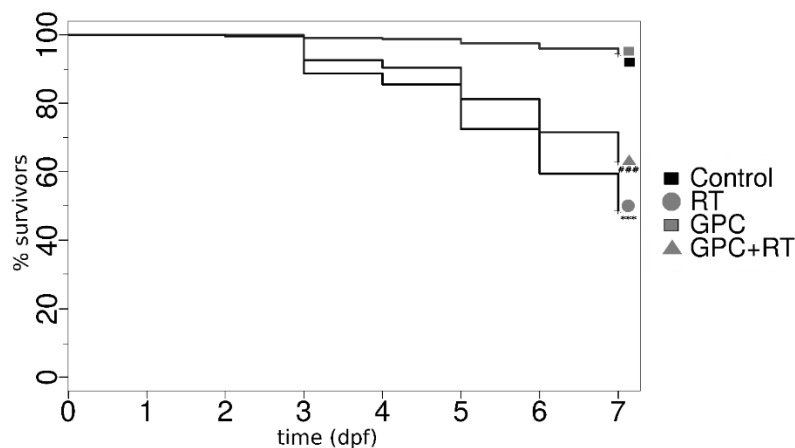


**Figure 12.** The effects of ionizing radiation on zebrafish survival in the presence of GPC. Zebrafish embryos at 24 hpf were mock irradiated (Control), mock irradiated in the presence of GPC (GPC), and irradiated with 20 Gy (RT) or 20 Gy in the presence of GPC (GPC+RT). \*\*\* $p < 0.001$  relative to the control group. #### $p < 0.001$  relative to the irradiated group.

##### 4.2.1. Histological evaluation

Radiation-induced cell damage of the different organ systems revealed that the most severe deterioration occurred at higher dose levels and there was an important radio-protective effect of GPC. In the groups irradiated with 20 Gy, large amounts of mucous and catarrhal were observed in the intestinal tract, and goblet cells were found in the intestinal mucous membrane. The effects of

radiation doses higher than 15 Gy caused irregular cell shape and larger hyperchromatic nuclei. These were characterized by pseudo-multilayer epithelia and moderate disorganization of the columnar cells and the cytoplasm was wider in the intestinal lumen. These severe alterations, induced by IR in the developing gastrointestinal system were reduced and partially restored by GPC pre-treatment (Figure 13).

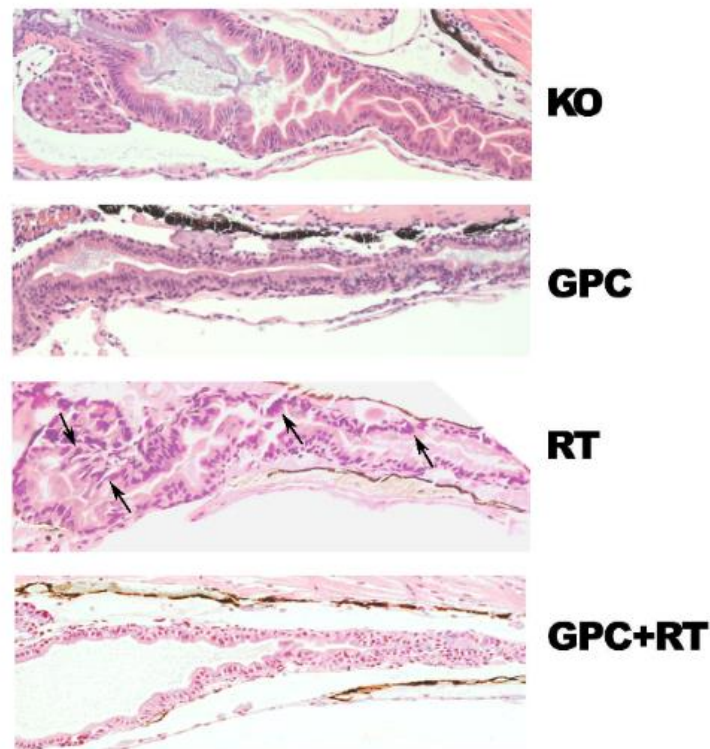


**Figure 13.** The effects of GPC on radiation-caused alterations of the gastrointestinal system. Representative histological sections of the intestine at 7 dpf, arrows (→) indicate the disorganization of the columnar cells in the intestinal lumen. Embryos at 24 hpf were pretreated with 194  $\mu\text{M/L}$  for 3 hours before irradiation with 20 Gy.

#### 4.2.2. Inflammatory cytokine level measurement

Whilst investigating the early phase of pro-inflammatory activation signal pathway it was found that the IL-1 $\beta$  expression (Figure 14(a)) was reduced to the control level in the pretreated group and thus the induction of the NF- $\kappa$ B pathway activation (Figure 14(b)) had been prevented.

The results show that IL-1 $\beta$  and NF- $\kappa$ B are activated in response to injury at different times, when measured 1 hour and 2 hours after 10 Gy irradiation. This activation level was reduced significantly by GPC.

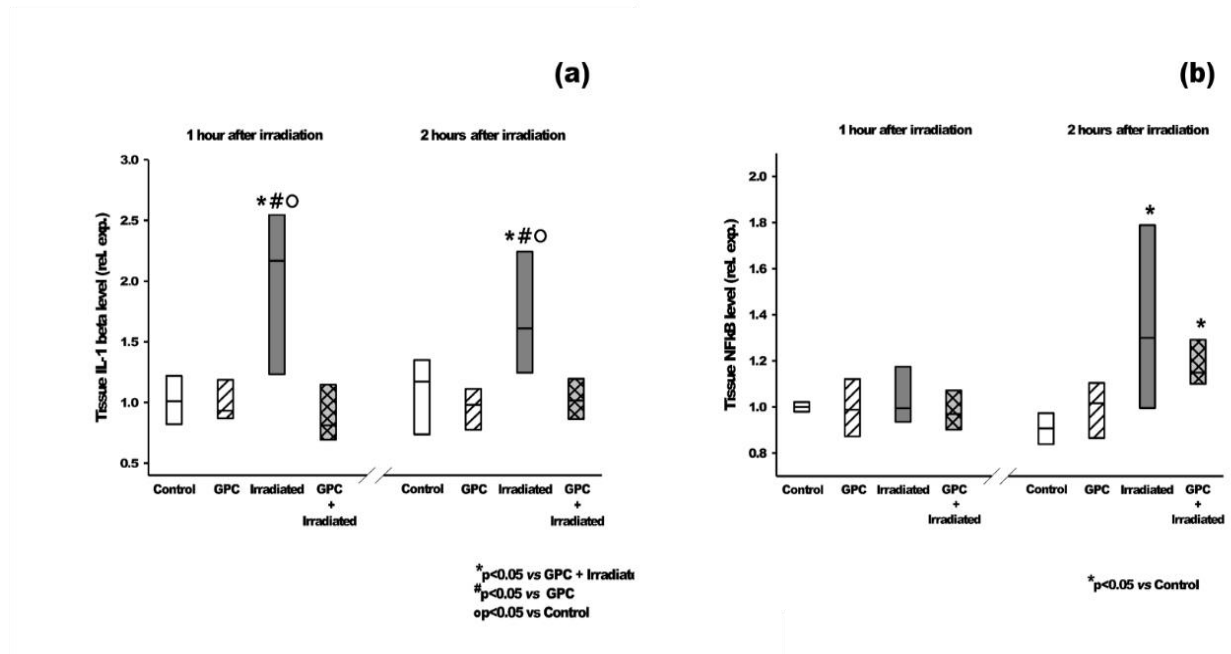


**Figure 14.** (a) Tissue IL-1 beta level relative expression, 1 hour and 2 hours after irradiation shows the effects of the mock irradiation, GPC treated mock irradiation, irradiation (10 Gy) and GPC treatment with irradiation (10 Gy). The symbol \* $p < 0.05$  relative to GPC treated and irradiated group. #  $p < 0.05$  relative to the GPC treated group. °  $p < 0.05$  relative to control group. (b) Tissue NF- $\kappa$ B level changes for the mock irradiation control group, the GPC treated mock irradiated group, the irradiated group (10 Gy) and the GPC treated irradiated group (10 Gy). The tissue NF- $\kappa$ B level at 2 hours after irradiation was significantly higher than the control group. \* $p < 0.05$  relative to the control group.

#### 4.3. Survival for high LET-RBE definition

Survival rates declined from the 4<sup>th</sup> dpi, with an increasing level of neutrons exposure resulting in an acceleration of the process. Survival was 90-100% for mock irradiated embryos. On the last observation day (7<sup>th</sup> dpi) significant differences were detected between the control groups and the 20 Gy (photon), 1.875 Gy, 2 Gy, 2.5 Gy (fission neutron), 8.12 Gy and 10.28 Gy (cyclotron based fast neutron) irradiated groups (Figure 15). The analysis of the survival curves resulted in LD<sub>50/7</sub> values of 2 Gy for fission neutrons, 8.12 Gy for cyclotron neutrons and 20 Gy for  $\gamma$  rays respectively. The ratio of the LD<sub>n/50/7</sub> for fission neutrons and LD <sub>$\gamma$ /50/7</sub> photon beam provided an RBE of 10 and for LD<sub>n/50/7</sub> 18 MeV neutrons and LD <sub>$\gamma$ /50/7</sub> reference photons of 2.5 (Figure 15).

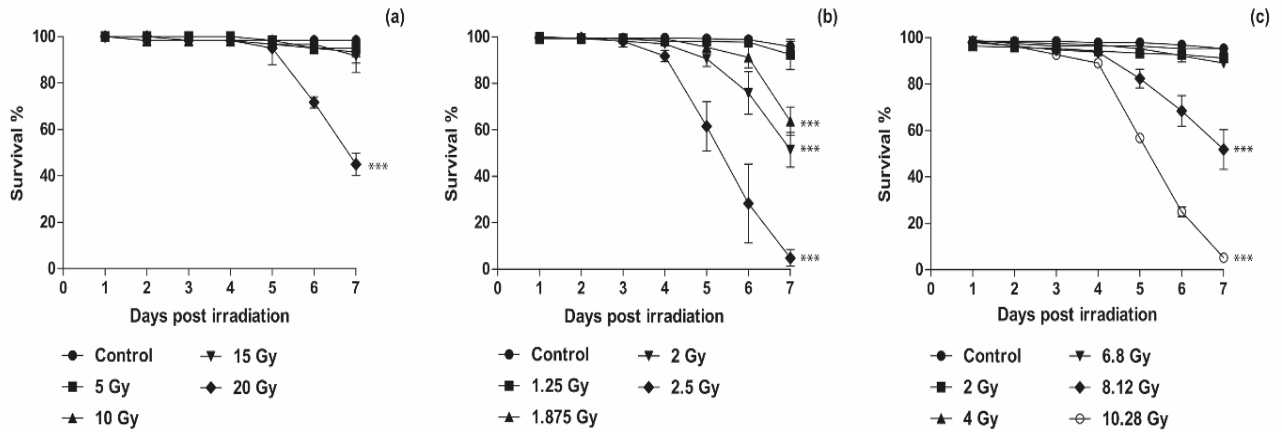


**Figure 15.** Dose dependent survival curves of zebrafish embryos. (a) Embryos at 24 hour post fertilization (hpf) were exposed to conventional photon with doses: 0 Gy (Control ●), 5 Gy (■), 10 Gy (▲), 15 Gy (▼), 20 Gy (◆). In the same developmental stages, embryos were treated with reactor fission neutrons (b) at dose levels 0 Gy (Control ●), 1.25 Gy (■), 1.875 Gy (▲), 2 Gy (▼), 2.5 Gy (◆) and (c) with cyclotron based fast neutron with 0 Gy (Control ●), 2 Gy (■), 4 Gy (▲), 6.8 Gy (▼), 8.12 Gy (◆), 10.28 Gy (○). Standard errors of the three independent experiments are included in the graphs; \*\*\* $p < 0.001$  significant differences relative to the control group.

#### 4.3.1. RBE determination by malformation

Developmental retardation and morphological changes (micro-ophthalmia, spine curvature, pericardial edema) of the living embryos were recorded with a simplified approach. Dose and LET dependent morphological changes were observed (Figure 16). The distortion assessment on the 4<sup>th</sup> and 5<sup>th</sup> dpi provided evaluable data for different radiation quality comparison which is in accordance with the survival based calculations. Using 24 hours observation periods, an exact definition of RBE is not possible, because of the steep dose distortion curve elevation of each radiation modality from 4<sup>th</sup> to 5<sup>th</sup> dpi.

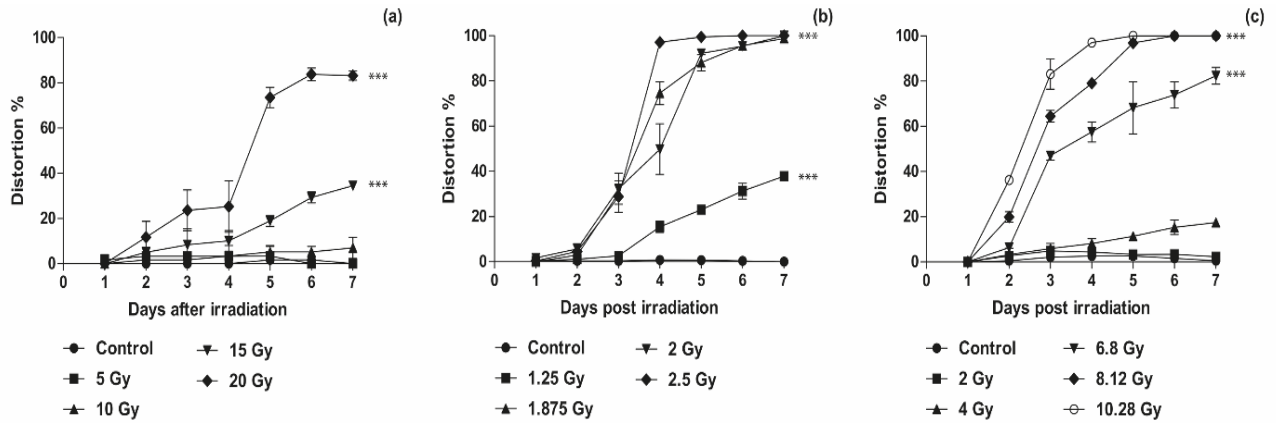


**Figure 16.** Daily assessment of morphologic changes after ionizing radiation treatment. (a) Embryos exposed to conventional photon with doses: 0 Gy (Control ●), 5 Gy (■), 10 Gy (▲), 15 Gy (▼), 20 Gy (◆). (b) Radiation with reactor fission neutrons at dose levels 0 Gy (Control ●), 1.25 Gy (■), 1.875 Gy (▲), 2 Gy (▼), 2.5 Gy (◆) and (c) with cyclotron based fast neutron with 0 Gy (Control ●), 2 Gy (■), 4 Gy (▲), 6.8 Gy (▼), 8.12 Gy (◆), 10.28 Gy (○). Results shows the represent mean  $\pm$ SD of triplicate experiments.

#### 4.3.2. Histopathology evaluation of different organs

The histopathological assessment showed tissue alterations in different organs (eye, brain, the gastrointestinal system, liver and muscles) of the embryos after IR. Microcephaly and microphthalmia were observed post irradiation and where the result of the downregulation of the cyclin D1 protein (Duffy *et al.*, 2005). At 7 day post treatment the volume of the eyes and the structure of its layers were analyzed in the coronal sections of the survived embryos. For evaluation the largest eye-diameter sections, was chosen from each treatment group (control and irradiated), where the lens was in the same plane. The different LET ionizing radiation treatments caused considerable disorganization of the retinal layers, in contrast to the separable cellular layers. The normal zebrafish embryo retina cellular organization is as follows: ganglion cell layer (gcl), inner plexiform layer (ipl), inner nuclear layer (inl), outer plexiform layer (opl), outer nuclear layer (onl), retinal pigmented epithelium (rpe) (Figure 17(a)). The two plexiform layer (ipl, opl) was difficult to distinguish or nearly disappeared in some individuals from the neutron irradiated group (Figure 17 white arrows). Independently on radiation quality the retinal pigmented epithelium (rpe) was specifically thickened (Figure 17(b)(d)). After irradiation the shape of the cells and its layers structures showed alteration, the prominent round nuclei of the inner and outer nuclear layer as well as the ganglion cell layer could not be discerned especially with increased dose levels.

The radiation resulted in lens opacification and the loss of volume (Figure 17(c)(d) white triangle). A remarkable decrease was observed in the diameter of the eye  $200.58 \pm 21 \mu\text{m}$  was in case of photon irradiation,  $210.98 \pm 32 \mu\text{m}$  and  $159.43 \pm 12 \mu\text{m}$  in embryos irradiated with fission neutron and cyclotron based neutron sources, compared to the control  $321.76 \pm 23 \mu\text{m}$  (Figure 17(a)(b)(c)(d)). In case of the brain of control embryos the neuropil is intact unlike in 20 Gy photon, 2 Gy groups using fission neutron and 8.12 Gy treated groups with cyclotron based neutron sources where neuropil loosening were observed. The low dose irradiation caused mild oedema in several observed individuals brain, independent of the radiation and pronounced cytotoxic oedema and neuropil vacuolization were detected in groups irradiated with higher doses. In the diencephalon (Figure 17(f)- white circle) and in the medulla (Figure 17(h)- white circle) cell disorganization was found 7 days after treatment in the individuals exposed to 20 Gy photon and 8.12 Gy cyclotron based neutron sources. The brain showed neuropil vacuolization in medulla (Figure 17(g)- white circle) and less perturbation in case of fission neutron irradiation with 2 Gy dose.

The radiation led to tissue disorganization and subsequent micro-erosion in the gastrointestinal system. In the groups irradiated with 20 Gy photon and 2 Gy fission neutron (Figure 18(b)(c)) the number of goblet cells partially decreased and in case of cyclotron based neutron at 8.12 Gy dose level (Figure 18(d)) they were almost completely depleted.

Histological analysis showed dose dependent lesions in the liver and tissue loosening and disorganization in the treated groups (Figure 18(b)(c)(d) white circle). In the neutron irradiation group's aggressive necrosis in the hepatocytes were found (Figure 18(c)(d)).

After neutron irradiation hypereosinophilic necrotic muscle-fibers and aggressive necrosis were detected in the muscles (Figure 18(b)(c)(d)). Dose dependent tissue alterations were detected in different organ systems, in the gastrointestinal mucosa, the cell lines were unsettled, the cells stained darkly and the nuclei were not basally located. The goblet cells particularly showed early signs of the effects of radiation and their number seemed to be well correlated to the delivered dose. The tissue damages caused by high LET radiation were more pronounced at the same dose level corresponding to LD<sub>50</sub> dose equivalent and it underlines the importance of an endpoint definition for RBE calculation.

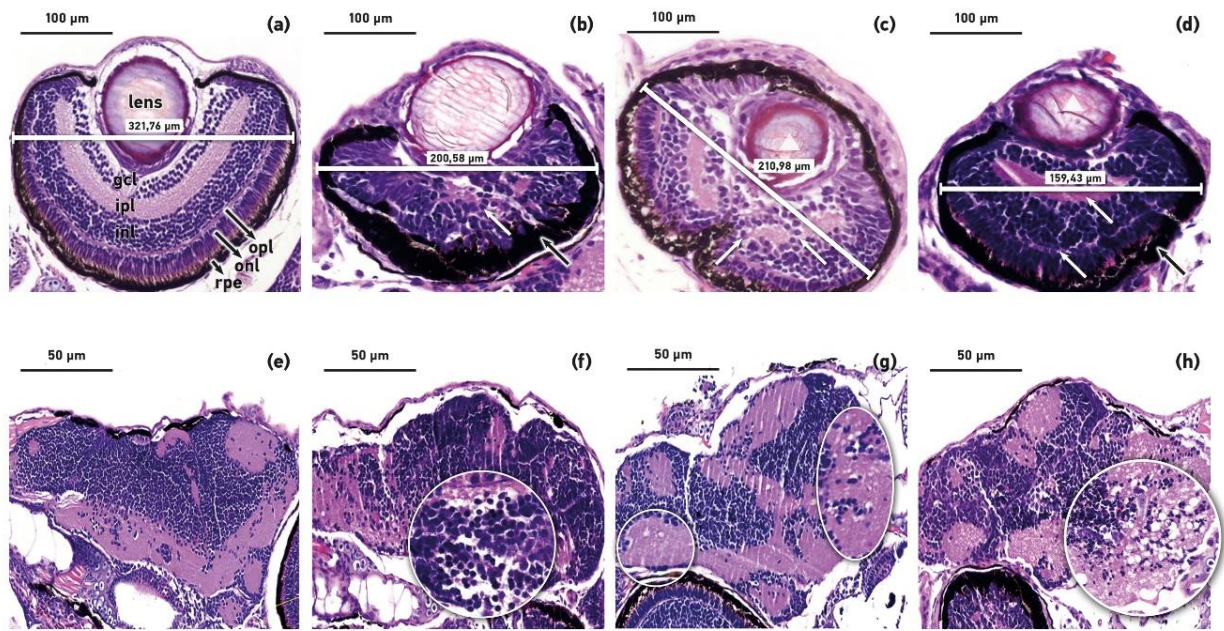


**Figure 17.** The effects of ionizing radiation in the eye and the developing central nervous system in zebrafish embryos. Representative H&E stained images of the eyes ((a)- control, (b)- photon 20 Gy, (c)- fission neutron 2 Gy, (d)- cyclotron based neutron 8.12 Gy) and the cranial structures of the brain ((e)-control, (f)-photon 20 Gy, (g)- fission neutron 2 Gy, (h)- cyclotron based neutron 8.12 Gy) of representative surviving zebrafish embryos at 168 hpf after exposure. (a) shows the different layers: lens; ipl and opl, inner and outer plexiform layer; gcl, ganglion cell layer; inl and onl, inner and outer nuclear layer; rpe, retinal pigmented epithelium. (20x magnification, scale bar 100 μm). The eye of neutron beam treated embryos shows loss of the lens volume and opacification of its ((c) (d) white triangle), other structures such as inner and outer plexiform layer ((b)(c)(d) white arrows) are difficult to distinguish or disappeared. The retinal pigmented epithelium shows thickening ((b)(d) black arrows). The treated embryos brain showed tissue disorganization in medulla and in the optic chiasm ((g)-white circle). There was a reduction in the level of the cell organization in the diencephalon ((f)-white circle) and in the medulla ((h)- white circle) in the observed individuals exposed with photon and cyclotron based neutron sources. 40x magnification, scale bar 50 μm.

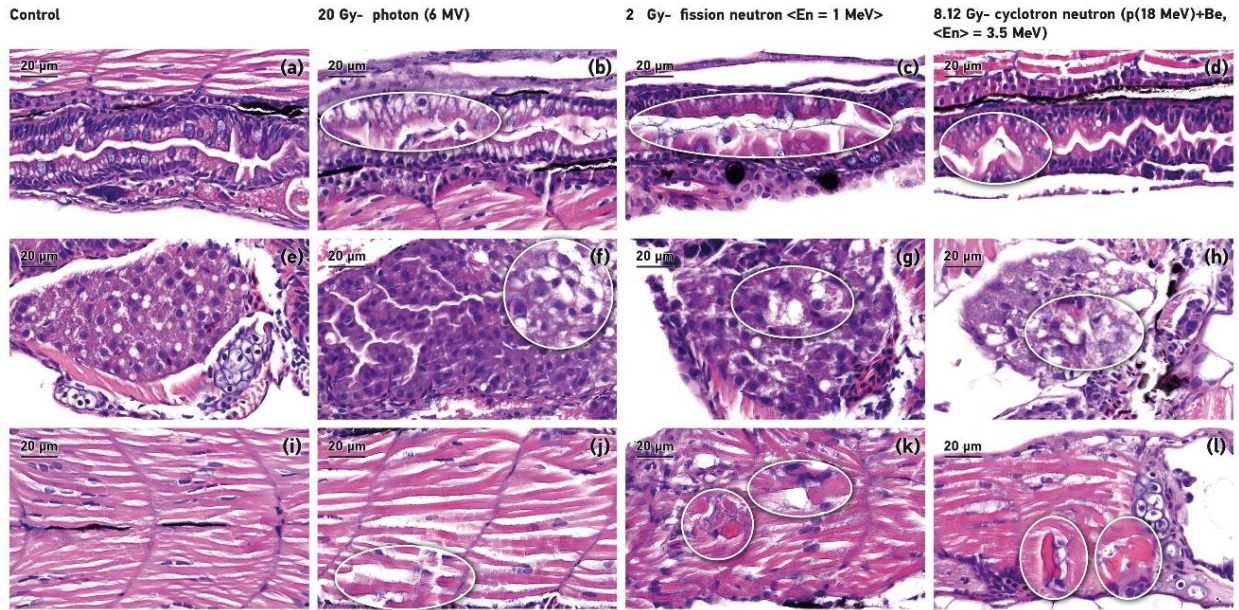


**Figure 18.** Different tissue radiation-induced alterations. Representative sagittal sections of the intestinal tract ((a)(b)(c)(d)), liver ((e)(f)(g)(h)) and the muscle ((i)(j)(k)(l)) from irradiated zebrafish embryos. There is a reduction in the number of goblet cells in the gastrointestinal system in all irradiated groups irrespectively of the radiation type ((b)(c)(d) beaded sections). In (f), (g), (h) white circles indicates tissue loosening, cell disorganization and hepatocytes necrosis (c) in the liver. (j), (k), (l) circle marked shows hypereosinophilic muscle-fibers and aggressive necrosis in the muscle. All images have an 80x magnification and scale bar is 50  $\mu\text{m}$ .

### 4.3.3 Proton treatment - RBE determination

#### 4.3.3.1 RBE by survival analysis

Dose-dependent survival curves (Figure 19) were determined by correlating the number of living embryos to the number of irradiated embryos of the respective day. On the first two days post irradiation (dpi) no significant impact was observed on embryonic survival for any doses and for doses lower than 15 Gy. Proton doses higher than 10 Gy for SOBP and 15 Gy for plateau irradiation significantly reduced survival levels at 4 dpi relative to the photon reference. This was also reflected in the  $\text{LD}_{50}$ , which was about 30 Gy for SOBP protons and slightly higher for plateau protons, whereas for photons considerably higher doses are required. Dose dependent RBE values ( $\pm$  standard error) calculated on basis of the obtained survival rates 4 dpi with protons of the mid-SOBP and the entrance plateau relative to 6 MV photons are shown in Table 1.

	mid-SOBP	plateau
RBE <sub>30Gy</sub> ± se	1.60 ± 0.32	1.41 ± 0.08
RBE <sub>20Gy</sub> ± se	1.20 ± 0.04	1.13 ± 0.08

**Table 1.** RBE values obtained for the two proton radiation qualities.

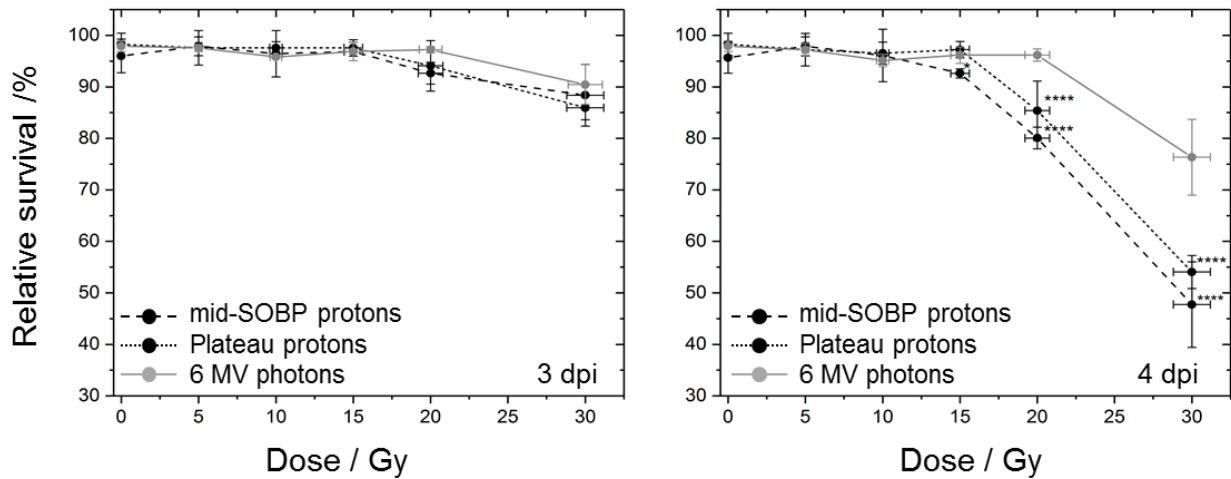


**Figure 19.** Relative embryo survival rates at 3<sup>rd</sup> and 4<sup>th</sup> dpi with plateau and mid-SOBP protons relative to the survival after 6 MV photon reference irradiation. Statistical significant differences to the photon reference are marked by \*\*\*\* ( $p < 0.0001$ ).

#### 4.3.3.2 RBE by malformation analysis

At the 1<sup>st</sup> dpi, there were just a few embryos with pericardial edema and spine deformations were observed in high dose (> 20 Gy) treatments. The number of malformations increased day by day, but doses below 15 Gy were less efficient in inducing malformations within 4 dpi. The number of embryos with pericardial edema, as one of the acute reactions after irradiation, increased faster than the number of embryos with spine bending (Figure 20). At the 2<sup>nd</sup> and 3<sup>rd</sup> dpi and for doses of 15 Gy and 20 Gy for the different radiation qualities significant differences in the rates of pericardial edema between proton and photon treatment were predominantly found (Figure 20). Doses higher than 15 Gy triggered pericardial edema in almost every treated embryo and a significant difference was found for the 15 Gy mid-SOBP irradiation group at the 4<sup>th</sup> dpi.

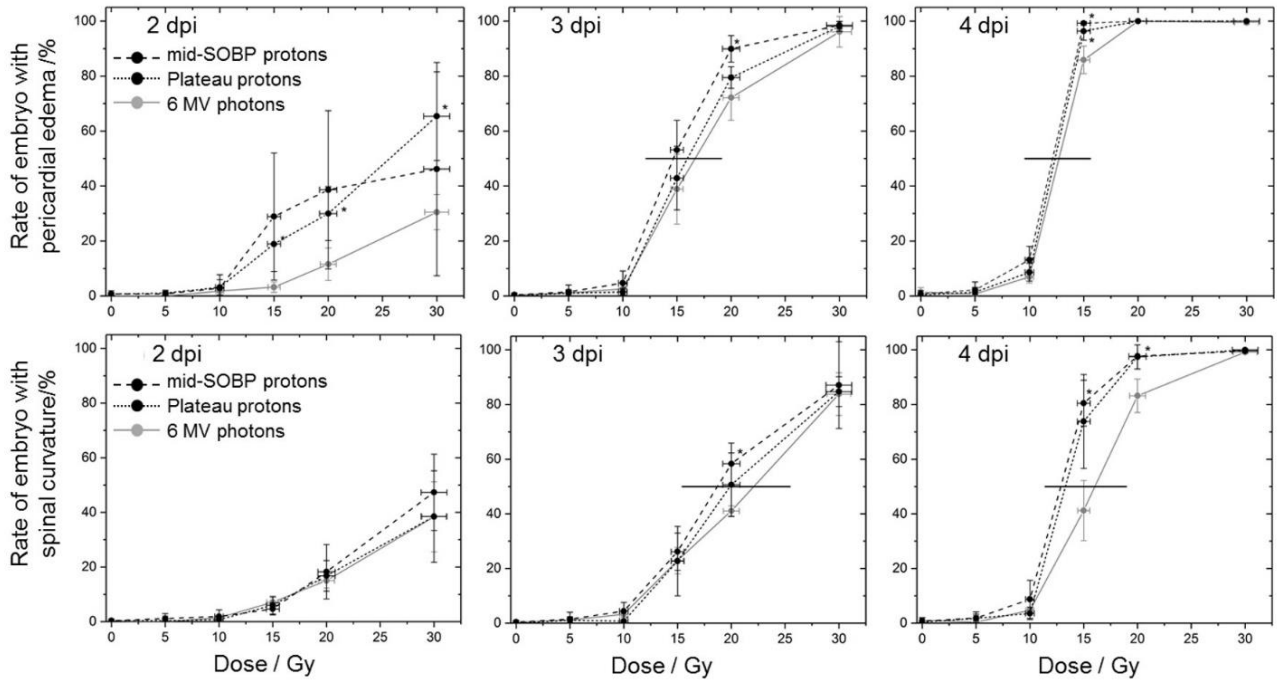


**Figure 20.** Time and dose-dependent development of pericardial edema and spine curvature for zebrafish embryo irradiation with 6 MV photons, proton plateau and mid-SOBP position (mean $\pm$ SD,  $p < 0.05$ ). Horizontal lines in the plots are shown to illustrate the differences in dose to induce 50% effect rate at 3<sup>rd</sup> and 4<sup>th</sup> dpi.

Comparing the malformation frequencies, at 4 dpi almost 100% of larvae treated with higher doses than 15 Gy exhibit pericardial edema, whereas a higher dose (30 Gy) was required to cause spine curvature in almost all embryos (Figure 20).

For the induction of pericardial edema a dose distinction of 12.9 Gy for proton and 16.0 Gy for photon treatment was found at the 3<sup>rd</sup> dpi, one day later a radiation quality independent dose of 12.5 Gy was measured (Figure 20, right). For comparison, distinct dose levels of 18.6 - 22.1 Gy at the 3<sup>rd</sup> dpi and of 14.7 - 16.7 Gy at the 4<sup>th</sup> dpi were measured for spine deformations in 50% of the embryos after proton relative to photon treatment. On basis of the spinal curvature rates observed 4 dpi with 20 Gy protons RBE values of  $1.25 \pm 0.16$  and of  $1.10 \pm 0.14$  were calculated for the exposure in mid-SOBP and entrance plateau region relative to MV photons, respectively. At 3<sup>rd</sup> dpi a proton quality independent RBE of  $1.17 \pm 0.10$  could be derived for 20 Gy treatments. Radiation quality alone does not result in significant differences regarding the qualitative assessment of the severity of the induced malformations at 3<sup>rd</sup> and 4<sup>th</sup> dpi, but a trend towards less severe damage only transitionally observed 3 dpi with photons (Figure 21).

Sigmoidal dose response curves became manifest for the pericardial edema as one example of acute radiation damage during the 4 day observation period. For spine curvature, a linear dose dependent

increase of severity up to dose of 30 Gy was observed at 4<sup>th</sup> dpi probably caused by extensive cell death in the spine for doses above 10 Gy.

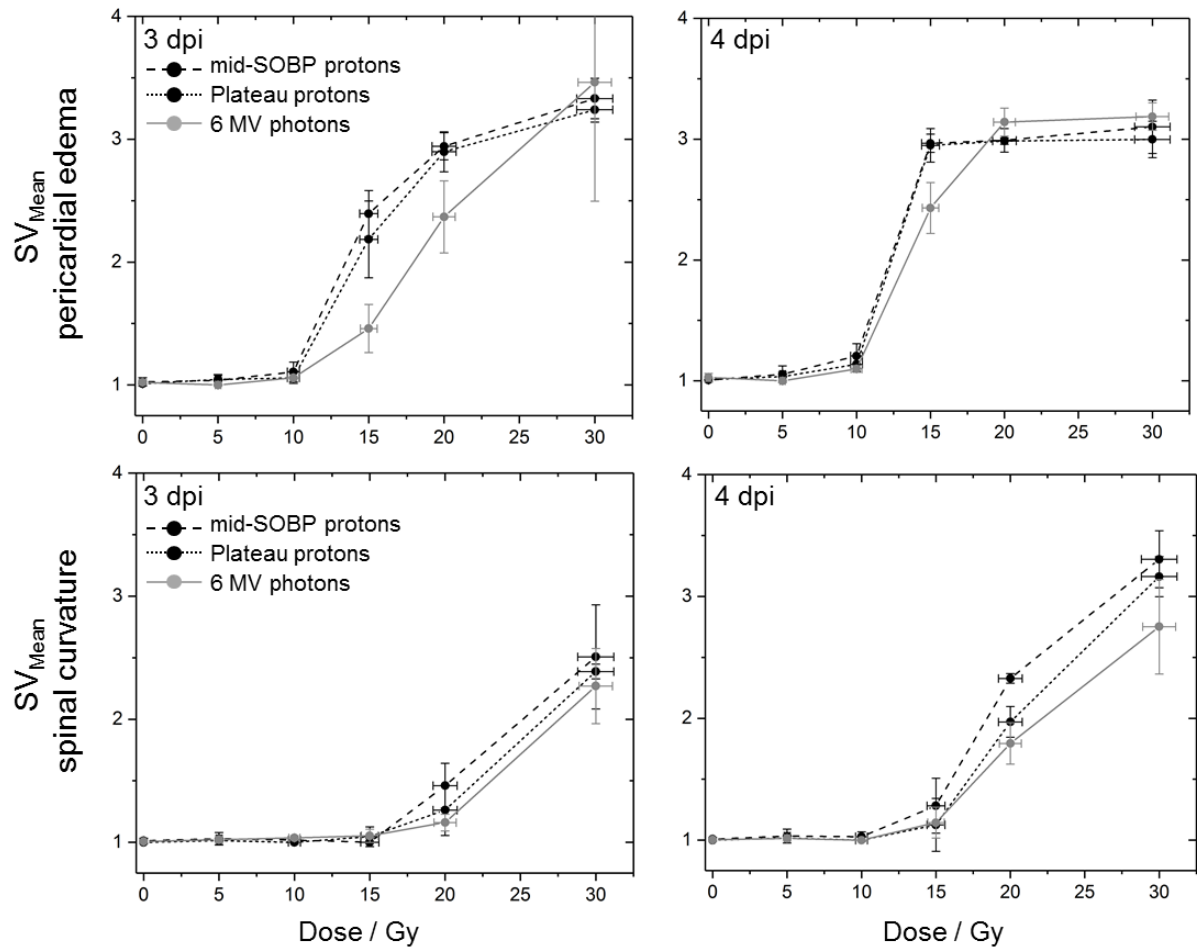


**Figure 21.** Mean scoring values describing the severity of the induced pericardial edema (upper row) and spine curvatures (lower row) at the 3<sup>rd</sup> and 4<sup>th</sup> dpi with mid-SOBP or plateau protons and 6 MV photons (mean $\pm$ SD,  $p < 0.05$ ).

## 5. DISCUSSION

The increasing use of particle therapy and the emergence of innovative radiation methods raise the necessity of valid, reproducible preclinical data on the biological effects of these ionizing radiations.

### 5.1. *Age and dose-dependent survival curves*

Few results have been published on fish embryo models (medaka, zebrafish) and they were used mainly for investigating on radiation protection aspects. Results - similarly to our findings – showed that the embryo mortality as well as the rate of morphological aberrations increased with higher radiation dose, but decreased with advanced embryonic age and maturity (Geiger *et al.*, 2006). Younger embryos, especially before midblastula transition (MBT) i.e. at the age < 24 hpf were found to have not yet fully developed radiation damage repair proteins (McAleer *et al.*, 2005), resulting in increased radiosensitivity, which was also confirmed by our experiments. Whereas the LD<sub>50</sub> was 20 Gy for embryos irradiated with standard photon beam at 24 hpf, a dose of only 15 Gy caused embryonic mortality of half of the embryos on the 7<sup>th</sup> dpi in the group irradiated at 6 hpf. These findings are consistent with the results of our experiments repeated several times, despite different photon sources being used for dose delivery. This strongly underlines that the zebrafish embryo model is highly suitable for radiation biology experiments. For further experiments with radiation modifying agents we set the dose to 20 Gy and used embryos of 24 hpf.

### 5.2. *Testing of potential radiation modifier*

Phospholipids play a major role in rearrangement and reduction of toxicity against agents damaging the cell membrane but about the direct toxicity of administrated phospholipids at high concentrations little is known. GPC is a phospholipid derivative known to stabilize cell membrane function after inflicting damage, which statement proved to be true in our investigation. GPC reduced the rate, alleviated the number and severity of morphological abnormalities (shortened and curved bodies, pericardial edema, malformations of the head and eye), when administered before radiation treatment. Histopathological slides showed, that especially the radiation damage to the gastrointestinal tract was greatly reduced and even partially restored to normal with GPC pre-treatment. As Westerfield (2000) described, major functional damage to the gastrointestinal system, like in the case of irradiation, will lead to death by starvation within 10 days after conception. GPC pre-treated embryos though, may be able to keep their normal nutritional capability. The GPC provided protection against radiation-induced overall lethality and damage to multiple organ systems. The reduction of edema in developing zebrafish demonstrated the protective effect as well. There is an evidence that the activation of canonical NF- $\kappa$ B pathway

plays a significant role in inflammatory changes induced by radiation in normal tissues in the developing vertebrate organism. The hypothesis of radioprotection by inhibiting inflammatory modulators like NF- $\kappa$ B was confirmed in the zebrafish model, in which the NF- $\kappa$ B inhibitors ethylpyruvate and the synthetic triterpenoid CDDO-TFEA were given in combination with radiation (Daroczi *et al.*, 2009). Therefore the NF- $\kappa$ B and IL-1 $\beta$  gene expression was studied, assuming that the observed protective effect of GPC may be due to the inhibition of this pathway. The essential pro-inflammatory cytokine of interleukin-1 family members (Vojtech *et al.*, 2012) the IL-1 $\beta$  is rapidly induced after irradiation and this cytokine has also been implicated in edema shaping (Gaber *et al.*, 2003, Mohanty *et al.*, 1989). Overexpression of IL-1 $\beta$  is the first sign of inflammatory activation after IR, which induces the activation of the NF- $\kappa$ B pathway (Ogryzko *et al.*, 2014). In the early radiation response the role of the NF- $\kappa$ B pathway activation has already been clearly established (Di Maggio 2015). The addition of GPC reduced the IL-1 $\beta$  expression down to the control level and prevented the activation of the NF- $\kappa$ B pathway. Transgenic mouse model studies failed due to the high mortality of the mouse embryos with abnormal function of NF- $\kappa$ B pathway or were biased due to compensatory molecular process activity. The zebrafish embryo proved to be a reliable model to study the effect of NF- $\kappa$ B pathway modulation on radiation response (Daroczi *et al.*, 2009, Hanisch *et al.*, 2004). Observation of modulation of early pro-inflammatory activation by GPC at a non-toxic concentration may provide an explanation for the radio-protective effect of the agent.

### **5.3. RBE determination of different high LET neutron sources**

The RBE is known to be variable and influenced by different factors such as tissue type, biological endpoint, treatment regimen, ion type (Lühr *et al.*, 2017). There has been a considerable amount of research performed in order to measure the RBE at different high LET sources at particle accelerator facilities worldwide using *in vitro* cell cultures, the gold standard of radiobiology (Kuhne *et al.*, 2009, Beyreuther *et al.*, 2009, Jones *et al.*, 2011, Seth *et al.*, 2014, Baiocco *et al.*, 2016, Jones, 2016). In order to overcome the uncertainties of the *in vitro* experiments, *in vivo* systems that are clinically more relevant have been introduced in radiation research providing important data on the dose dependent reactions of a complex organism. Rodent species (mice, rats) models have been established as *in vivo* examinations models using special quantitative and semi-quantitative endpoints. Van der Kogel *et al.* (2002) introduced the rat spinal cord model which was also used in larger animals (Medin *et al.*, 2011). Gueulette *et al.* (2001) performed large inter-comparison studies for RBE definition at different facilities generating fast neutrons, epithermal neutrons based BNCT and proton beams using the Lieberkühn crypt test on mice. Further acute radiation effects are assessed using of the rodent lung pneumonitis assay, delayed skin reaction scoring and rat spinal cord damage (assessed by hind leg

motion depletion), mouse skin and kidney irradiation (Joiner, 1989, Van der Kogel *et al.*, 2002, Uzawa *et al.*, 2007, Lühr *et al.*, 2017). Numerous experiments have been performed for determination of high-LET-RBE in mice and rabbit models (Hamada and Sato, 2016, Ainsbury *et al.*, 2016) using lens opacification as an endpoint. For quantitative assessment of the biological effectivity of high LET radiation with changing parameters (dose rate, fractionation) and for inter-comparison of different non-conventional facilities and specific biological properties of different ion species (Joiner *et al.*, 1983, Dokic *et al.*, 2016) these rodent model based tests proved to be reproducible and reliable.

The development of a less vulnerable, and less expensive novel *in vivo* vertebrate model, which fulfills the requirements drawn up by E. J. Hall (1979) to be a “convenient, portable and reproducible” biological system for inter-comparison, is essential for studies on emerging radiation modalities. Few reports have been published on neutron RBEs using fish embryo model by assessment of different endpoints (Wang *et al.*, 2011, Epperly *et al.*, 2012, Ng *et al.*, 2015, Ng *et al.*, 2016). Shima *et al.* (1991) introduced specific locus mutation assay in germ cell lines for measuring the RBE of fission neutrons resulting a value in between 3-7, using the Japanese medaka fish embryos. Takai *et al.* (2004) published dose and time dependent responses for micronucleus induction in gill cells of medaka with irradiation of X-rays and fast neutrons defining an RBE of  $4.3 \pm 0.6$ .

RBE definition of high LET beams relied on two quantitative endpoints (survival and malformation) and a detailed tissue damage histological analysis resulted in similar results obtained using another fish species with different endpoint assessment. In line with results published by other *in vivo* models for fast neutron beams, in our experiments the RBE defined by zebrafish embryo survival, increases with decreasing neutron energy (from - 2.5 for p(18 MeV)+Be to - 10 for 1 MeV fission neutrons). This energy dependence of biological effect of neutron beams is far well known (Baiocco *et al.*, 2016, Bateman *et al.*, 1961, Hall *et al.*, 1975, Field, 1976). We have observed that the 1 MeV mean energy mixed neutron-photon beam proved to be 4 times more effective biologically than the 18 MeV mean energy mixed neutron-photon radiation. The result of the calculated RBE values was well supported by the experiments performed using broad energy spectra, mixed neutron-photon and monoenergetic neutron beams (Juerß *et al.*, 2017). The high reliability of the zebrafish embryo survival assay was revealed during the repeated neutron irradiation experiments, therefore, survival analysis is considered as reliable tool for RBE measurements. Detected microscopic changes (marked cellular changes in eyes, brain, liver, muscle and in the gastrointestinal system) were more pronounced at higher dose levels and at higher LET radiations similar to the results of the survival comparison. All of the investigated tissues in the literature, the tail muscle, intestinal tract, central nerve system and eye exhibited clearly identifiable radiation related alterations, i.e. hypocellularity and disorganization of cellular layers in concordance with these findings.

#### 5.4. *Biological effects of proton beam*

The radiobiological effects along the charged particle path at two positions could be investigated with high spatial resolution due to their small size of about 0.5 - 1 mm. Consistent with the observation of Freeman *et al.* (2014) the hatching rates observed in this study after irradiation during pharyngula period show no significant dependence on radiation quality and dose, and other publications also show a rather unaffected hatching rate after radiation treatment (McAleer *et al.*, 2005, Hu *et al.*, 2016, Kumar *et al.*, 2017). A few exceptions were published, they observed lower hatching rates two days after irradiation of 24 hpf embryos with 1 Gy of  $^{137}\text{Cs}$  gamma irradiation and 12 Gy of 8 MeV protons (Hu *et al.*, 2016 and Li *et al.*, 2018).

The survival of 24 hpf zebrafish embryos was not reduced significantly by doses up to 15 Gy of MV photons and protons at the entrance of plateau, and by up to 10 Gy at mid-SOBP protons respectively. The number of surviving embryos significantly declines at higher doses, for proton treatment more efficient than for photons, whereas for protons the delivery of 30 Gy resulted in a 50% survival rate (LD<sub>50</sub>) already at the 4<sup>th</sup> dpi in our work. The dose threshold of 15 Gy for embryonic mortality observed at 4 dpi was also seen by others (McAleer *et al.*, 2005), whereas for lower energy protons of 8 MeV higher mortality rates were already revealed 4 days after treatment of 24 hpf wild type embryos with a dose of 6 Gy (Li *et al.*, 2018). Since 8 MeV protons have a range of about 0.8 mm in water (Berger *et al.*, 2005) therefore in the experiment of Li *et al.* (2018) zebrafish embryos were predominantly treated with high LET radiation which correlated to a significantly increased RBE and their observation supported that at 3 Gy dose the normal development of the 24 hpf embryo is significantly altered. Survival rates and the analysis of morphological abnormalities revealed that doses higher than 10 Gy were required to trigger pericardial edema and spinal curvature within the follow up time of four days. Similar threshold doses of about 10 Gy were observed at 4 dpi in embryos treated during pharyngula stage with 60 Co  $\gamma$ -rays (Freeman *et al.*, 2014).

Pervasive and fast appearance of pericardial edema correlates with its emergence as acute inflammation reaction induced by cytokines released early after irradiation (Schaue *et al.*, 2012). In contrast, deformations of the spine are probably caused by the apoptosis of neuronal cells in the developing spinal cord (Sayed and Mitani, 2016), which takes time to cause observable abnormalities after irradiation.

As a result of excessive experimental campaign by assessment of survival RBE values of  $1.13 \pm 0.08$  and of  $1.20 \pm 0.04$  were obtained relative to the clinical MV photon beam at 4 dpi with 20 Gy of plateau and mid-SOBP protons, respectively. This has not been realized so far with aquatic animals. These values are in accordance with RBE values in the range of 0.96 - 1.13 and of 1.0 - 1.2 found in previous *in vivo* studies for treatments in the entrance plateau and mid-SOBP position (Urano *et al.*,

1984, Uzawa *et al.*, 2007, Saager *et al.*, 2018). Several *in vitro* experiments have been performed in order to resolve the RBE-LET dependency with higher spatial resolution, the increased RBE of  $1.41 \pm 0.08$  and of  $1.60 \pm 0.32$  for 30 Gy exposures at the respective positions rather matched RBE values found in cellular survival studies at the distal end of the proton path (Chaudhary *et al.*, 2014, Paganetti, 2014, Ilicic *et al.*, 2018), whereby the achievement of the LD<sub>50</sub> at this dose point might also have an influence on the validity of the derived RBE. The biological effects do not only depend on radiation quality, but also on species, dose fractionation, tissue or cell type, endpoint, timing, therefore all these points should be considered in the general comparability of RBE data. In this context, a comparison of RBE obtained on basis of zebrafish embryonic survival rates to other *in vivo* results, which are most often based on measurements of acute or late effects of a single organ in rodents is critical (Saager *et al.*, 2017, 2018; Sørensen *et al.*, 2017). The attempt to derive RBE values on the basis of the different malformations found at 4 dpi was feasible so far only for the spinal curvature, however pericardial edema as an acute reaction was observed in all embryos, with saturation effect. For the rates of spinal curvature RBE values of  $1.25 \pm 0.16$  and of  $1.10 \pm 0.14$  were revealed after treatment in mid-SOBP and entrance plateau position, which are comparable to those obtained on the basis of the embryonic survival rates and to RBE values determined by other *in vivo* models.

In conclusion, our study validates the general applicability of zebrafish embryo as an alternative small vertebrate model for testing and assessing different radiation qualities even under non-laboratory conditions. Qualitative endpoints such as survival and malformations can be used to describe the overall effect of radiation on the whole organism. The potential application of zebrafish embryos for spatially resolved RBE measurements along the proton depth dose distribution seems to be conceivable.

## 6. CONCLUSION AND FINDINGS

- a) We have founded the first Zebrafish laboratory in Szeged and we have contributed significantly to the establishment of a novel vertebrate model for radiobiology research. The fish embryo system proved to be appropriate for investigating the effects of different ionizing radiation on a large scale and for preclinical studies on potential radio-protective agents.
- b) Exact and controlled dose delivery techniques and adapted radiation setup of zebrafish embryos for special technical conditions including limitations had been worked out.
- c) The proper embryonal age, observation time points for assessment of the different biologic endpoints, such as survival, reliable quantitative morphological analysis, and complex evaluation of histopathologic and molecular changes could be defined. We derived well-reproducible dose-response curves and LD<sub>50</sub> for each radiation quality.
- d) In our experiments GPC exhibited protective effects against radiation induced lethality, multi-organ morphological and histological impairment. Our results suggest that the inhibition of early radiation induced activity of pro-inflammatory pathway activation could be a potential mode of action of GPC. GPC may therefore be a possible future candidate for protection of the normal tissues exposed to incident IR during cancer radiotherapy.
- e) Viability and malformation detection has been shown to be a responsive measure for all radiation types. We have defined the RBE for fission and cyclotron based neutron as well as for proton sources.
- f) The potential application of zebrafish embryos for spatially resolved RBE measurements along the proton depth dose distribution proved to be conceivable.

We have achieved a relevant step toward validation and optimization of a novel vertebrate model for future radiobiological research on LDI beams. Further powerful endpoints and complex quantitative assessments are under evaluation.

## 7. ACKNOWLEDGEMENTS

First of all, I would like to express my sincere gratitude to my supervisor, Katalin Hideghéty M.D., Ph.D., Habil. Associate Professor at the Department of Oncotherapy, University of Szeged and Group Leader of Biomedical Application Group at ELI-ALPS, for giving me the opportunity to work as a researcher. I am very grateful for her continuous support during my Ph.D. study and research activity, for her scientific advices and her sustained trust in me. Without her continuous support, never-failing interest and optimistic attitude to the scientific problems, this Ph.D. study could hardly have been completed.

I would like to express my thanks to my colleagues and friends to Dr. Imola Plangár and Dr. Tünde Tókécs for their support and help at the beginning of my career, during my work for their friendship and that they supported me in good and bad times.

I owe especial thanks to Dr. rer.nat. Jörg Pawelke, for giving me the opportunity to participate in several experimental campaign joining the OncoOptics group. I am very grateful to have allowed the zebrafish embryos irradiation studies with conventional and laser driven proton beams, and for his help during the experimental preparatory work and dosimetry measurements, and of course for his advices. It was a great pleasure for me to work with him.

My special thanks to Dr. Elke Beyreuther, for her lot of efforts during the preparation and execution in our joint experiments. I am very grateful for her personal guidance and advices. Her selfless help of writing the manuscript, and last but not least for her friendship.

From the University of Szeged I owe thanks to Dr. Ferenc Bari for his support, and for giving the opportunity to develop our Zebrafish lab in his Institution. Thanks to Dr. József Kaszaki, for giving me the possibility to hold lecture in some courses which I learned a lot from.

Thanks to colleagues from the Department of Aquaculture, Szent István University, for their support and advices, and many thanks for providing to our disposal the adult zebrafish stock.

I owe special thanks to ELI-HU Nonprofit Ltd. leaders, here I would highlight Károly Osvay and the Scientific Application Division head, Péter Dombi, who have made my doctoral studies possible. During my research work, I got a lot of help and support from Vera Zimányiné Horváth, Zita Váradi and Renáta Ékesné Balogh.

I would like to thank to my students Ákos Diódsi, Dr. Maria Kalinger and Evelin Polanek for their assistance work and friendship. I wish to express my special gratitude to my family and friends for believing in me, for their endless support and love during my work.

Last, but most importantly, I am very grateful to my groom, Szabolcs Ruzsa, who has sustained, encouraged and supported me with love several times during my studies.

*The ELI-ALPS project (GINOP-2.3.6-15-2015-00001) is supported by the European Union and co-financed by the European Regional Development Fund. The project has received funding from the European Union's Horizon 2020 research and innovation program under grant agreement no 654148 Laserlab-Europe.*

## 8. REFERENCES

1. Ainsbury EA, Barnard S, Bright S, Dalke C, Jarrin M, Kunze S, Tanner R, Dynlacht JR, Quinlan RA, Graw J, Kadhim M, Hamada N. Ionizing radiation induced cataracts: Recent biological and mechanistic developments and perspectives for future research. *Mutat Res* 2016; 770: 238-261.
2. Allemani C, Weir HK, Carreira H, Harewood R, Spika D, Wang XS, Bannon F, Ahn JV, Johnson CJ, Bonaventure A, Marcos-Gragera R, Stiller C, Azevedo e Silva G, Chen WQ, Ogunbiyi OJ, Rachet B, Soeberg MJ, You H, Matsuda T, Bielska-Lasota M, Storm H, Tucker TC, Coleman MP;CONCORD Working Group. Global surveillance of cancer survival 1995-2009: analysis of individual data for 25,676,887 patients from 279 population-based registries in 67 countries (CONCORD-2). *Lancet* 2015; 385: 977-1010.
3. Amaldi U, Kraft G. Radiotherapy with beams of carbon ions. *Reports on Progress in Physics* 2005; vol. 68, nr.8.
4. Amatruda JF, Shepard JL, Stern HM, Zon LI. Zebrafish as a cancer model system. *Cancer Cell* 2002; 1: 229-31.
5. Amenta F, Liu A, Zeng YC, Zaccheo D. Muscarinic cholinergic receptors in the hippocampus of aged rats: influence of choline alfoscerate treatment. *Mech Ageing Dev* 1994; 76: 49-64.
6. Bailey JM, Creamer BA, and Hollingsworth MA. What a Fish Can Learn from a Mouse: Principles and Strategies for Modeling Human Cancer in Mice. *Zebrafish* 2009; 6: 329-37.
7. Baiocco G, Barbieri S, Babini G, Morini J, Alloni D, Friedland W, Kunderát P, Scmitt E, Puchalska M, Sihver L and Ottolenghi A. The origin of neutron biological effective as a function of energy. *Sci Rep* 2016; 6: 34033.
8. Barbagallo SG, Barbagallo M, Giordano M, Meli M, Panzarasa R. alpha-Glycerophosphocholine in the mental recovery of cerebral ischemic attacks. *Ann N Y Acad Sci* 1994; 30: 253-69.
9. Barriuso J, Nagaraju R, Hurlstone A. Zebrafish: a new companion for translational research in oncology. *Clin Cancer Res* 2015; 21: 969-75.
10. Barth RF, Vicente MG, Harling OK, Kiger WS 3rd, Riley KJ, Binns PJ, Wagner FM, Suzuki M, Aihara T, Kato I, Kawabata S. Current status of boron neutron capture therapy of high grade gliomas and recurrent head and neck cancer. *Radiat Oncol* 2012; 7: 146.

11. Baskar R, Kuo Ann Lee, Richard Yeo and Kheng-Wei Yeoh. Cancer and Radiation Therapy: Current Advantages and Future Discussions. *Int J Med Sci* 2012; 9: 193-199.
12. Bateman JL, Rossi HH, Bond VP, Gilmartin J. The dependence of RBE on energy of fast neutrons. 2. Biological evaluation of discrete neutron energies in the range 0.43 to 1.80 Mev. *Radiat Res* 1961; 15: 694-706.
13. Beasley M, Driver D, Dobbs H J. Complications of radiotherapy: improving the therapeutic index. *Cancer Imaging* 2005; 5: 78–84.
14. Berger MJ, Coursey JS, Zucker MA, Chang J ESTAR, PSTAR, and ASTAR: Computer Programs for Calculating Stopping-Power and Range Tables for Electrons, Protons, and Helium Ions (version 1.2.3). National Institute of Standards and Technology, Gaithersburg, MD 2005.
15. Beyreuther E, Baumann M, Enghardt E, Helmbrecht S, Karsch L, Krause M, Pawelke J, Schreiner L, Schürer M, von Neubeck C, Lühr A. Research facility for radiobiological studies at the University Proton Therapy Dresden. *Int J Particle Ther* 2018; 5: 172-182.
16. Beyreuther E, Dörr W, Lehnert A, Lessmann E and Pawelke J. Relative biological effectiveness of 25 and 10 kV X-rays for the induction of chromosomal aberrations in two human mammary epithelial cell lines. *Radiat Environ Biophys* 2009; 48: 333-40.
17. Bijl HP, van Luijk P, Coppens RP, Schippers JM, Konings AW, Van der Kogel AJ. Dose-volume effects in the rat cervical spinal cord after proton irradiation. *Int J radiation Oncol Biol Phys* 2002; 52: 205-11.
18. Bladen C, Navarre S, Dynan W, Kozlowski D. Expression of the Ku70 subunit (XRCC6) and protection from low dose ionizing radiation during zebrafish embryogenesis. *Neurosci Lett* 2007; 422: 97-102.
19. Blank KR, Rudoltz MS, Kao GD, Muschel RJ, McKenna WG. The molecular regulation of apoptosis and implications for radiation oncology. *Int J Radiat Biol* 1997; 71: 455-466.
20. Brannen KC, Panzica-Kelly JM, Danberry TL, Augustine-Rauch KA. Development of a zebrafish embryo teratogenicity assay and quantitative prediction model. *Birth Defects Res B Dev Reprod Toxicol* 2010; 89: 66-77.
21. Bräuer-Krisch E, Adam JF, Alagoz E, Bartzsch S, Crosbie J, DeWagter C, Dipuglia A, Donzelli M, Doran S, Fournier P, Kalef-Ezra J, Kock A, Lerch M, McErlean C, Oelfke U, Olko P, Petasecca M, Povoli M, Rosenfeld A, Siegbahn EA, Sporea D, Stugu B. Medical physics aspects of the synchrotron radiation therapies: Microbeam radiation therapy (MRT) and synchrotron stereotactic radiotherapy (SSRT). *Phys Med* 2015; 31: 568-83.

22. Broerse J J, Mijnheer BJ and Williams JR. European protocol for neutron dosimetry for external beam therapy. *British Journal of Radiology* 2014; 54: 882-898.
23. Brownawell AM, Carmines EL, Montesano F. Safety assessment of AGPC as a food ingredient. *Food Chem Toxicol* 2011; 49: 1303-15.
24. Chaudhary P, Marshall TI, Perozziello FM, Manti L, Currell FJ, Hanton F, McMahon SJ, Kavanagh JN, Cirrone GA, Romano F, Prise KM, Schettino G. Relative biological effectiveness variation along monoenergetic and modulated Bragg peaks of a 62-MeV therapeutic proton beam: a preclinical assessment. *Int J Radiat Oncol Biol Phys* 2014; 90: 27-35.
25. Daroczi B, Kari G, McAleer MF, Wolf JC, Rodeck U and Dicker AP. In vivo radioprotection by the fullerene nanoparticle DF-1 as assessed in a zebrafish model. *Clin Cancer Res.* 2006; 12: 7086-91.
26. Daroczi B., Kari G., Ren Q., Dicker A., Rodeck U. NF- $\kappa$ B inhibitors alleviate and the proteasome inhibitor PS-341 exacerbates radiation toxicity in zebrafish embryos. *Mol Cancer Ther* 2009; 8: 2625-2634.
27. De Jesus Moreno, Moreno M. Cognitive improvement in mild to moderate Alzheimer's dementia after treatment with the acetylcholine precursor choline alfoscerate: a multicenter, double-blind, randomized, placebo-controlled trial. *Clin Ther* 2003; 25: 178-193.
28. Di Maggio FM, Minafra L, Forte GI, Cammarata FP, Lio D, Messa C, Gilardi MC, Bravata V. Portrait of inflammatory response to ionizing radiation treatment. *J Inflamm (Lond)* 2015; 12: 14.
29. Dokic I, Mairani A, Niklas M, Zimmermann F, Chaudhri N, Kronic D, Tessonnier T, Ferrari A, Parodi K, Jäkel O, Debus J, Haberer T, Abdollahi A. Next generation multi scale biophysical characterization of high precision cancer particle radiotherapy using clinical proton, helium-, carbon- and oxygen ion beams. *Oncotarget* 2016; 7: 56676-56689.
30. Drago F, Mauceri F, Nardo L, Valeris C, Lauria N, Rampello L, Guidi G. Behavioral effects of L-alpha-glycerolphosphorylcholine: influence on cognitive mechanisms in the rat. *Pharmacol Biochem Behav* 1992; 41: 445-448.
31. Duffy KT, McAleer MF, Davidson WR, Kari L, Kari C, Liu CG, Farber SA, Cheng KC, Mest JR, Wickstrom E, Dicker AP, Rodeck U. Coordinate control of cell cycle regulatory genes in zebrafish development tested by cyclin D1 knockdown with

- morpholino phosphorodiamidates and hydroxypropyl-phosphono peptide nucleic acids. *Nucleic Acids Res* 2005; 33: 4914–4921.
32. Epperly MW, Bahary N, Quader M, Dewald V, Greenberger JS. The zebrafish- *Danio rerio*-is a useful model for measuring the effects of small-molecule mitigators of late effects of ionizing irradiation. *In Vivo* 2012; 26: 889-897.
  33. Erős G, Ibrahim S, Siebert N, Boros M, Vollmar B. Oral phosphatidylcholine pretreatment alleviates the signs of experimental rheumatoid arthritis. *Arthritis Res Ther* 2009; 11: 43.
  34. Fenyvesi A. Neutron sources for basic and applied research at the MGC-20E cyclotron of Atomki. *Proceedings of the Enlargement Workshop on Neutron Measurements and Evaluations for Applications. NEMEA. Centre Institute for Reference Materials and Measurements* 2004; 68-74.
  35. Field SB. An historical survey of radiobiology and radiotherapy with fast neutrons. *Curr Top Radiat Res Q* 1976; 11: 1-86.
  36. Freeman JL, Weber GJ, Peterson SM, Nie LH. Embryonic ionizing radiation exposure results in expression alterations of genes associated with cardiovascular and neurological development, function, and disease and modified cardiovascular function in zebrafish. *Front Genet* 2014; 5: 268.
  37. Gaber MW, Sabek OM, Fukatsu K, Wilcox HG, Kiani MF, Merchant TE. Differences in ICAM-1 and TNF-alpha expression between large single fraction and fractionated irradiation in mouse brain. *Int J Radiat Biol* 2003; 79: 359–366.
  38. Gallazzini M, Burg MB. What's new about osmotic regulation of glycerophosphocholine. *Physiology* 2009; 24: 245–249.
  39. Geiger GA, Fu W, Kao GD. Temozolomide-Mediated Radiosensitization of Human Glioma Cells in a Zebrafish Embryonic System. *Cancer Res* 2008; 68: 3396-3404.
  40. Geiger GA, Parker SE, Beothy AP, Tucker JA, Mullins MC, Kao GD. Zebrafish as a “Biosensor”? Effects of Ionizing Radiation and Amifostine on Embryonic Viability and Development. *Cancer Res* 2006; 66: 8172-81.
  41. Gera L, Varga R, Török L, Kaszaki J, Szabó A, Nagy K, Boros M. Beneficial effects of phosphatidylcholine during hindlimb reperfusion. *J Surg Res* 2007; 139: 45-50.
  42. Ghyczy M, Torday C, Kaszaki J, Szabó A, Czóbel M, Boros M. Oral phosphatidylcholine pretreatment decreases ischemia-reperfusion-induced methane generation and the inflammatory response in the small intestine. *Shock* 2008; 30: 596-602.
  43. Gould SJ. *Ontogeny and Phylogeny*. Harvard University Press, Cambridge 1977.

44. Gueulette J, Böhm L, De Coster BM, Vynckier S, Octave-Prignot M, Schreuder AN, Symons JE, Jones DTL, Wambersie A, Scalliet P. RBE variation as a function of depth in the 200-MeV proton beam produced at the National Accelerator Centre in Faure (South Africa). *Radiother Oncol* 1997; 42: 303-309.
45. Gueulette J, Slabbert JP, Böhm L, De Coster BM, Rosier JF, Octave-Prignot M, Ruifrok A, Schreuder AN, Wambersie A, Scalliet P, Jones DT. Proton RBE for early intestinal tolerance in mice after fractionated irradiation. *Radiother Oncol* 2001; 61: 177-84.
46. Hall EJ and Kellerer A. Review of RBE data for cell in culture. In *High LET radiations in Clinical Radiotherapy*. Pergamon Press Ltd, Headington Hill Hall, Oxford, England 1979; 171-174.
47. Hall EJ, Giaccia AJ. *Radiobiology for the radiologist*. Lippincott Williams & Wilkins, 6th edition, Philadelphia 2006; 5-28, 47-58, 103-115, 129-153, 293-330, 378-429, 460-463.
48. Hall EJ, Novak JK, Kellerer AM, Rossi HH, Marino S, Goodman LJ. RBE as a function of neutron energy. I. Experimental observations. *Radiat Res* 1975; 64: 245-55.
49. Hamada N, Sato T. Cataractogenesis following high-LET radiation exposure. *Mutat Res* 2016; 770: 262-291.
50. Hanisch UK, van Rossum D, Xie Y, Gast K, Misselwitz R, Auriola S, Goldsteins G, Koistinaho J, Kettenmann H, Möller T. The microglia-activating potential of thrombin: the protease is not involved in the induction of proinflammatory cytokines and chemokines. *J Biol Chem* 2004; 279: 51880-51887.
51. Helmbrecht S, Baumann M, Enghardt W, Fiedler F, Krause M, Lühr A. Design and implementation of a robust and cost-effective double-scattering system at a horizontal proton beamline. *J Instrum* 2016; 11.
52. Hendry JH, West CM. Apoptosis and mitotic cell death: their relative contributions to normal-tissue and tumour radiation response. *Int J Radiat Biol* 1997; 71: 709-719.
53. Hideghéty K, Szabó ER, Polanek R, Szabó Z, Ughy B, Brunner S, Tókécs T. An evaluation of the various aspects of the progress in clinical applications of laser driven ionizing radiation. *Journal of Instrumentation* 2017; vol. 2.
54. Hu M, Hu N, Ding D, Zhao W, Feng Y, Zhang H, Li G, Wang Y. Developmental toxicity and oxidative stress induced by gamma irradiation in zebrafish embryos. *Radiat Environ Biophys* 2016; 55: 441-450.
55. Hurem S, Martin LM, Brede DA, Skjerve E, Nourizadeh-Lillabadi R, Lind OC, Christensen T, Berg V, Teien HC, Salbu B, Oughton DH, Aleström P, Lyche JL. Dose-

- dependent effects of gamma radiation on the early zebrafish development and gene expression. *PLoS ONE* 2017; 12.
56. Hwang M, Yong C, Moretti L and Lu B. Zebrafish as a model system to screen radiation modifiers. *Curr Genomics* 2007; 8: 360-369.
  57. Ilicic K, Combs SE, Schmid TE. New insights in the relative radiobiological effectiveness of proton irradiation. *Radiat Oncol* 2018; 13: 6.
  58. Jarvis R., Knowles J. DNA damage in zebrafish larvae induced by exposure to low-dose rate  $\gamma$ -radiation: detection by the alkaline comet assay. *Mutat Res Toxicol Environ Mutagen* 2003; 541: 63–69.
  59. Joiner M, van der Kogel A. *Basic Clinical Radiobiology*. 4th edition. London, United Kingdom: Hodder Arnold 2009.
  60. Joiner MC, Maughan RL, Fowler JF and Denekamp J. The RBE for mouse skin irradiated with 3-MeV neutrons: single and fractionated doses. *Radiat Res* 1983; 95: 130-141.
  61. Joiner Mc. A comparison of the effects of p(62)+Be and d(16)+Be neutrons in mouse kidney. *Radiother Oncol* 1989; 13: 211-214.
  62. Jones B, Dale RG, Deehan C, Hopkins KI and Morgan DA. The role of biologically effective dose (BED) in clinical oncology. *Clin Oncol (R Coll Radiol)* 2001; 13: 71-81.
  63. Jones B, Underwood TS, Carabe-Fernandez A, Timlin C, Dale RG. Fast neutron relative biological effects and implications for charged particle therapy. *Br J Radiol* 2011; 1: 11-18.
  64. Jones B. Why RBE must be a variable and not a constant in proton therapy. *Br J Radiol* 2016; 89: 1063.
  65. Juerß D, Zwar M, Giesen U, Nolte R, Kriesen S, Baiocco G, Puchalska M, van Goethem MJ, Manda K, Hildebrandt G. Comparative study of the effects of different radiation qualities on normal human breast cells. *Radiat Oncol* 2017; 12: 159.
  66. Kalifa, C., Grill, J. The Therapy of Infantile Malignant Brain Tumors: Current Status? *Journal of Neuro-Oncology* 2005; 75: 279-285.
  67. Kidd PM. Integrated Brain Restoration after Ischemic Stroke – Medical Management, Risk Factors, Nutrients, and other Interventions for Managing Inflammation and Enhancing Brain Plasticity. *Altern Med Rev* 2009; 14: 14-35.
  68. Kimmel CB, Ballard WW, Kimmel SR, Ullmann B, Schilling TF. Stages of embryonic development of the zebrafish. *Dev Dyn* 1995; 203: 253-310.

69. Komatsu H, Westerman J, Snoek GT, Taraschi TF, Janes N. L-alpha glycerylphosphorylcholine inhibits the transfer function of phosphatidylinositol transfer protein alpha. *Biochim Biophys Acta* 2003; 1635: 67-74.
70. Kuhne WW, Gersey BB, Wilkins R, Wu H, Wender SA, George V, Dynan WS. Biological effects of high-energy neutrons measured in vivo using a vertebrate model. *Radiat Res* 2009; 172: 473-480.
71. Kumar MKP, Shyama SK, Kashif S, Dubey SK, Avelyno D, Sonaye BH, Kadam Samit B, Chaubey RC. Effects of gamma radiation on the early developmental stages of Zebrafish (*Danio rerio*). *Ecotoxicol Environ Saf* 2017; 142: 95-101.
72. Langheinrich U. Zebrafish: a new model on the pharmaceutical catwalk. *Bioassays* 2003; 9: 904-912.
73. Larouche, V., Huang, A., Bartels, U., Bouffet, E. Tumors of the central nervous system in the first year of life. *Pediatric Blood & Cancer* 2007; 49: 1074-1082.
74. Levin WP, Kooy H, Loeffler JS, DeLaney TF. Proton beam therapy. *Br J Cancer* 2005; 93: 849-854.
75. Li X, Zha X, Wang Y, Jia R, Hu B, Zhao B. Toxic effects and foundation of proton radiation on the early-life stage of zebrafish development. *Chemosphere* 2018; 200: 302-312.
76. Liao JJ, Parvathaneni U, Laramore GE, Thompson JA, Bhatia S, Futran ND, Bhrany AD, Hawes SE, Ladra M. Fast neutron radiotherapy for primary mucosal melanomas of the head and neck. *Head Neck* 2014; 36: 1162-1167.
77. Livak KJ, Schmittgen TD. Analysis of relative gene expression data using real-time quantitative PCR and the 2(-Delta Delta C(T)). *Method Methods* 2001; 25: 402-408.
78. Lühr A, von Neubeck C, Helmbrecht S, Baumann M, Enghardt W, Krause M. Modeling in vivo relative biological effectiveness in particle therapy for clinically relevant endpoints. *Acta Oncol* 2017; 56: 1392-1398.
79. Lühr A, von Neubeck C, Pawelke J, Seidlitz A, Bentzen SM, Bortfeld TR, Debus J, Deutsch E, Langendijk HA, Loeffler JS, Mohan R, Scholz M, Sørensen BS, Weber DC, Krause M, Baumann M. "Radiobiology of Proton Therapy": results of an international expert workshop. *Radiother Oncol* 2018; 128: 56-67.
80. McAleer MF, Davidson C, Davidson WR, Yentzer B, Farber SA, Rodeck U, Dicker AP. Novel use of zebrafish as a vertebrate model to screen radiation protectors and sensitizers. *Int J Radiat Oncol Biol Phys* 2005; 61: 10-13.

81. Medin PM, Foster RD, van der Kogel AJ, Sayre JW, McBride WH, Solberg TD. Spinal cord tolerance to single-fraction partial-volume irradiation: a swine model. *Int J Radiat Oncol Biol Phys* 2011; 79: 226-232.
82. Meng H, Terado T, Kimura H. Apoptosis induced by X-rays and chemical agents in murine fibroblastic cell lines with a defect in repair of DNA double-strand breaks. *Int J Radiat Biol* 1998; 73: 503-510.
83. Mohanty S, Dey PK, Sharma HS, Singh S, Chansouria JP, Olsson Y. Role of histamine in traumatic brain edema. An experimental study in the rat. *J Neurol Sci* 1989; 90: 87-97.
84. Ng CY, Kong EY, Kobayashi A, Suya N, Uchihori Y, Cheng SH, Konishi T, Yu KN. Non-induction of radioadaptive response in zebrafish embryos by neutrons. *Radiat Res* 2016; 57: 210-219.
85. Ng CYP, Kong EY, Kobayashi A, Suya N, Uchihori Y, Cheng SH, Konishi T, Yu KN. Neutron induced bystander effect among zebrafish embryos. *Radiation Physics and Chemistry* 2015; 117: 153–159.
86. Ogryzko NV, Hoggett EE, Solaymani-Kohal S, Tazzyman S, Chico TJ, Renshaw SA, Wilson HL. Zebrafish tissue injury causes upregulation of interleukin-1 and caspase-dependent amplification of the inflammatory response. *Dis Model Mech* 2014; 7:259-264.
87. Olive PL, Durand RE. Apoptosis: an indicator of radiosensitivity in vitro?. *Int J Radiat Biol* 1997; 71: 695-707.
88. Onishchenko LS, Gaikova ON, Yanishevskii SN. Changes at the focus of experimental ischemic stroke treated with neuroprotective agents. *Neurosci Behav Physiol* 2008; 38: 49-54.
89. Paganetti H. Relative biological effectiveness (RBE) values for proton beam therapy. Variations as a function of biological endpoint, dose, and linear energy transfer. *Phys Med Biol* 2014; 59: 419-472.
90. Parnetti L, Mignini F, Tomassoni D, Traini E, Amenta F. Cholinergic precursors in the treatment of cognitive impairment of vascular origin: ineffective approaches or need for re-evaluation?. *J Neurol Sci* 2007; 257: 264-269.
91. Peeler CR, Mirkovic D, Titt U, Blanchard P, Gunther JR, Mahajan A, Mohan R, Grosshans DR. Clinical evidence of variable proton biological effectiveness in pediatric patients treated for ependymoma. *Radiother Oncol* 2016; 121: 395-401.
92. Peeters A, Grutters JP, Pijls-Johannesma M, Reimoser S, De Ruyscher D, Severens JL, Joore MA and Lambin P. How costly is particle therapy? Cost analysis of external beam radiotherapy with carbon-ions, protons and photons. *Radiother Oncol* 2010; 95: 45-53.

93. Pei DS, Strauss PR. Zebrafish as a model system to study DNA damage and repair. *Mutat Res* 2013; 743-744:151-159.
94. Plangár I, Szabó ER, Tókéš T, Mán I, Brinyiczki K, Fekete G, Németh I, Ghyczy M, Boros M, Hideghéty K. Radio-neuroprotective effect of L-alpha glycerylphosphorylcholine (GPC) in an experimental rat model. *J Neurooncol* 2014; 119: 253-261.
95. Prasad, K. *Handbook of Radiobiology*; CRC Press, 2nd edition, Boca Raton New York London Tokyo 1995; 1-6, 26-57, 117-118, 305-314.
96. Prasanna PGS, Stone HB, Wong R S, Capala J, Bernhard EJ, Vikram B, Coleman CN. Normal tissue protection for improving radiotherapy: Where are the Gaps?. *Transl Cancer Res* 2012; 1: 35–48.
97. Richter C, Pausch G, Barczyk S, Priegnitz M, Keitz I, Thiele J, Smeets J, Stappen FV, Bombelli L, Fiorini C, Hotoiu L, Perali I, Prieels D, Enghardt W, Baumann M. First clinical application of a prompt gamma based in vivo proton range verification system. *Radiother Oncol* 2016; 118: 232-237.
98. Rosenfeld AB, Wroe AJ., Cornelius IM., Reinhard M, Alexiev D. Analysis of Inelastic Interactions for Therapeutic Proton Beams Using Monte Carlo Simulation *IEEE Transactions on nuclear science* 2004; vol. 51, no. 6.
99. Saager M, Peschke P, Brons S, Debus J, Karger CP. Determination of the proton RBE in the rat spinal cord: Is there an increase towards the end of the spread-out Bragg peak?. *Radiother Oncol* 2018; 128: 115-120.
100. Saager M, Peschke P, Brons S, Scholz M, Huber PE, Debus J, Karger CP. Investigation of the RBE variation of protons in the rat spinal cord within a spread-out Bragg peak. *Radiother Oncol* 2017; 123: 273-274.
101. Sayed AE, Mitani H. The notochord curvature in medaka (*Oryzias latipes*) embryos as a response to ultraviolet A irradiation. *J Photochem Photobiol B* 2016; 164: 132-140.
102. Schae D, Kachikwu EL, McBride WH. Cytokines in radiobiological responses: a review. *Radiat Res* 2012; 178: 505-523.
103. Schüler E, Eriksson K, Hynning E, Hancock SL, Hiniker SM, Bazalova-Carter M, Wong T, Le QT, Loo BW Jr, Maxim PG. Very high-energy electron (VHEE) beams in radiation therapy; Treatment plan comparison between VHEE, VMAT and PPBS. *Med Phys* 2017; 44: 2544-2555.

104. Scribner DM, Witowski NE, Mulier KE, Luszczek ER, Wasiluk KR, Beilman GJ. Liver metabolomic changes identify biochemical pathways in hemorrhagic shock. *J Surg Res* 2010; 164: 131-139.
105. Seth I, Schwartz JL, Stewart RD, Robert Emery R, Joiner MC, Tucker JD. Neutron Exposures in Human Cells: Bystander Effect and Relative Biological Effectiveness. *PLoS One* 2014; 9: 98947.
106. Seymour C., Mothersill C. *New Developments in Fundamental and Applied Radiobiology*. Nuclear Energy Board of Ireland; Taylor & Francis, London New York 1991.
107. Shima A and Shimada A. Development of a possible nonmammalian test system for radiation-induced germ-cell mutagenesis using a fish, the Japanese medaka (*Oryzias latipes*). *Proc Natl Acad Sci USA* 1991; 88: 2545-2549.
108. Sørensen BS, Bassler N, Nielsen S, Horsman MR, Grzanka L, Spejlborg H, Swakoń J, Olko P, Overgaard J. Relative biological effectiveness (RBE) and distal edge effects of proton radiation on early damage in vivo. *Acta Oncol* 2017; 56: 1387-1391.
109. Specht HM, Neff T, Reuschel W, Wagner FM, Kampf S, Wilkens JJ, Petry W, Combs SE. Paving the Road for Modern Particle Therapy - What Can We Learn from the Experience Gained with Fast Neutron Therapy in Munich?. *Front Oncol* 2015; 5: 262.
110. Steel G. G. *Basic Clinical Radiobiology*. First published in Great Britain 1993.
111. Stern HM, Zon LI. Cancer genetics and drug discovery in the zebrafish. *Nat Rev Cancer* 2003; 3: 533-539.
112. Takai A, Kagawa N and Fujikawa K. Dose- and time dependent response for micronucleus induction by X-rays and fast neutrons in gill cells of medaka (*Oryzias latipes*). *Environ Mol Mutagen* 2004; 44: 108-112.
113. Tayebati SK, Tomassoni D, Di Stefano A, Sozio P, Cerasa LS, Amenta F. Effect of choline-containing phospholipids on brain cholinergic transporters in the rat. *J Neurol Sci* 2011; 302: 49-57.
114. Tőkés T, Erős G, Bebes A, Hartmann P, Várszegi S, Varga G, Kaszaki J, Gulya K, Ghyczy M, Boros M. Protective effects of a phosphatidylcholine-enriched diet in lipopolysaccharide-induced experimental neuroinflammation in the rat. *Shock* 2011; 36: 458-465.
115. Tőkés T, Tuboly E, Varga G, Major L, Ghyczy M, Kaszaki J, Boros M. Protective effects of L-alpha-glycerolphosphorylcholine on ischaemia-reperfusion-induced inflammatory reactions. *Eur J Nut* 2015; 54: 109-118.

116. Tókéš T, Varga G, Garab D, Nagy Z, Fekete G, Tuboly E, Plangár I, Mán I, Szabó RE, Szabó Z, Volford G, Ghyczy M, Kaszaki J, Boros M, Hideghéty K. Peripheral inflammatory activation after hippocampus irradiation in the rat. *Int J Radiat Biol* 2014; 90: 1-6.
117. Treede I, Braun A, Jeliaskova P, Giese T, Füllekrung J, Griffiths G, Stremmel W, Eehalt R. TNF- $\alpha$ -induced up-regulation of pro-inflammatory cytokines is reduced by phosphatidylcholine in intestinal epithelial cells. *BMC Gastroenterol* 2009; 13: 9-53.
118. Tubiana M, Dutreix J, Wambersie A. *Introduction to Radiobiology*. Taylor & Francis, London New York Philadelphia 1990; 273-300.
119. Urano M, Verhey LJ, Goitein M, Tepper JE, Suit HD, Mendiondo O, Gragoudas ES, Koehler A. Relative biological effectiveness of modulated proton beams in various murine tissues. *Int J Radiat Oncol Biol Phys* 1984; 10: 509-514.
120. Uzawa A, Ando K, Furusawa Y, Kagiya G, Fuji H, Hata M, Sakae T, Terunuma T, Scholz M, Ritter S, Peschke P. Biological intercomparison using gut crypt survivals for proton and carbon-ion beams. *J Radiat Res* 2007; 48: 75-80.
121. Vojtech LN, Scharping N, Woodson JC, Hansen JD. Roles of Inflammatory Caspases during Processing of Zebrafish Interleukin-1 in *Francisella noatunensis* Infection. *Infect Immun* 2012; 8: 2878-2885.
122. Volinsky R, Kinnunen PK. Oxidized phosphatidylcholines in membrane-level cellular signaling: from biophysics to physiology and molecular pathology. *FEBS J* 2013; 280: 2806–2816.
123. Wang C, Smith RW, Duhig J, Prestwich WV, Byun SH, McNeill FE, Seymour CB, Mothersill CE. Neutrons do not produce a bystander effect in zebrafish irradiated in vivo. *Int J Radiat Biol* 2011; 87: 964-973.
124. Warenus HM, Britten RA and Peacock JH. The relative cellular radiosensitivity of 30 human in vitro cell lines of different histological type to high LET 62.5 MeV (p-.Be1) fast neutrons and 4 MeV photons. *Radiother Oncol* 1994; 30: 83-89.
125. Westerfield M. *The Zebrafish Book, A guide for the laboratory use of zebrafish Danio rerio*. University of Oregon Press 2000; 4th edition.
126. Yasuda T, Kamahori M, Nagata K, Watanabe-Asaka T, Suzuki M, Funayama T, Mitani H and Oda S. Abscopal Activation of Microglia in Embryonic Fish Brain Following Targeted Irradiation with Heavy-Ion Microbeam. *Int J Mol Sci* 2017; 18: 1428.
127. Yoon DK, Jung JY, Suh TS. Application of proton boron fusion reaction to radiation therapy: A Monte Carlo simulation study. *Appl Phys Lett* 2014; 105: 223507.

128. Zeil K, Beyreuther E, Lessmann E, Wagner W, Pawelke J. Cell irradiation setup and dosimetry for radiobiological studies at ELBE. *NIM B* 2009; 267: 2403-2410.
129. Zindler JD, Thomas CR Jr, Hahn SM, Hoffmann AL, Troost EG, Lambin P. Increasing the Therapeutic Ratio of Stereotactic Ablative Radiotherapy by Individualized IsotoxicDose Prescription. *J Natl Cancer Inst* 2015; 108.
130. Zon LI. Zebrafish: a new model for human disease. *Genome Res* 1999; 9: 99-100.

**ANNEX 1.**

**Emília Rita Szabó**, Imola Plangár, Tünde Tőkés, Imola Mán, Róbert Polanek, Róbert Kovács, Gábor Fekete, Zoltán Szabó, Zsolt Csenki, Ferenc Baska, Katalin Hideghéty: L-alpha glycerylphosphorylcholine as a Potential Radioprotective Agent in Zebrafish Embryo Model. *Zebrafish* 2016; 13: 481-488.

**ANNEX 2.**

**Emília Rita Szabó**, Zita Reisz, Róbert Polanek, Tünde Tőkés, Szabolcs Czifrus, Csilla Pesznyák, Barna Biró, Fenyvesi A, Beáta Király, József Molnár, Borbála Daroczi, Szilvia Brunner, Zoltán Varga, Katalin Hideghéty: A novel vertebrate system for the examination and direct comparison of the relative biological effectiveness for different radiation qualities and sources. *International Journal of Radiation Biology* 2018;

**ANNEX 3.**

**Emília Rita Szabó**, Michael Brand, Stefan Hans, Katalin Hideghéty, Leonhard Karsch, Elisabeth Leßmann, Jörg Pawelke, Michael Schürer, Elke Beyreuther: Radiobiological effects and proton RBE determined by wildtype zebrafish embryos. *Plos One* (under review)

## EGYETEMI DOKTORI ÉRTEKEZÉS – MAGYAR NYELVŰ ÖSSZEFOGLALÓ

A sugárterápia a komplex rákkezelés egyik fő pillére. A sugárbiológia több évtizedes kutatásai alapján ma már sok mindent megismertünk az ionizáló sugárzásról. Hatásának megismerése nagymértékben hozzájárult az optimális alkalmazás kidolgozásához, amely mind a sugárvédelem fejlődését, mind széleskörű alkalmazását ezek között a sugárterápia hatékonyságának fokozását tette lehetővé, ami a terápiás index javulását eredményezte. Régóta ismert, hogy az ionizáló sugárzás közvetlen sejtkárosító hatásának fő célpontja az örökítő anyag, valamint hogy a sugárzás okozta sejtkárosodások a sejt típusától, a sugárzási körülményektől és a sugárzás minőségétől függően különböző mértékűek és jelentőségűek lehetnek. Vezethetnek a sejt halálához letális mutációkon keresztül, okozhatnak olyan szubletális károsodásokat, melyek összeadódva hosszabb idő elteltével eredményezhetik a sejt halálát, vagy elindíthatnak olyan károsító folyamatokat, melyeken keresztül a sugársérülést nem szenvedett egészséges sejtek, szövetek is sérülhetnek. Az új generációs lineáris gyorsítókkal elérhető intenzitás modulált sugárkezelések, a töltött részecskék kedvező dózis elnyelési tulajdonsága hozzájárul a malignus sejtek szelektív eliminálásához, a normál szövetműködés megőrzése mellett. A hadron terápiás alkalmazások gyors növekedése, megbízható *in vivo* modellek kifejlesztését igényli a nagy lineáris energiatranszfer (LET) részecske sugárzás biológiai hatásainak preklinikai vizsgálatához. Rendkívül fontos a korábbi empirikus klinikai eredmények pathomechanizmusának, molekuláris hátterének kutatása, valamint a különböző új sugárminőségek biológiai hatékonyságának tanulmányozása és az innovatív bináris és multimodális kezelési koncepciók együtthatásának feltérképezése, a daganat ellenes terápiák hatékonyságának növelése érdekében.

### **1. Zebradánió halembrió modell validálása a sugárbiológiai kutatásokhoz**

Kísérleteink célja az volt, hogy egy megbízható, reprodukálható, preklinikai állatmodellt tervezzünk és alkalmazzunk, ionizáló sugárzás által kiváltott biológiai hatások vizsgálatára, különböző potenciális sugármódosító vegyületek tanulmányozására, valamint Relatív Biológiai Effektivitás (RBE) meghatározására, speciális sugárforrások alkalmazásával.

A zebradánió (*Danio rerio*) halembrió népszerű gerinces modellé vált, mivel számos előnnyel rendelkezik a hagyományos állatmodellekkel szemben. Laboratóriumi körülmények között alacsony költség mellett könnyen szaporítható, fenntartható, valamint nagy reprodukciós képesség jellemzi őket. Az 0,5-1 mm-es embriók átlátszóságuk, és könnyű kezelhetőségük miatt kiválóan alkalmasak nagyszámú egyeddel történő vizsgálatok kivitelezésére. A kis méret nagy térbeli felbontást nyújt, a teljes organizmus nagyszámú egyedeinek besugárzása megbízható letalitási adatokat eredményez. A

zebradánió számos kulcsfontosságú génnel rendelkezik, amelyek fontos szerepet töltenek be a fejlődés folyamataiban, a sejtciklus, a proliferáció, valamint a differenciálódás során, ezek a gének megfelelnek a humán DNS szakaszoknak (70%) és jól konzerváltak a két faj között. A legtöbb szerv, mint például a szem, agy, szív, máj, izmok, csontok valamint a gyomor-bél rendszer gyors embrionális fejlődésen mennek keresztül, közel 48 óra alatt teljes fejlődésük végbemegy. Ezen túlmenően, a zebrahal embriók és a fiatal felnőtt egyedek optikailag áttetszőek, ez a jellegzetességük megkönnyíti az ionizáló sugárzás belső szervekre kifejtett hatásának közvetlen megfigyelését. Ezek mindegyike jelentős előnyt jelent a preklinikai kutatásban való alkalmazáshoz, és a munkánk során igen alkalmasnak bizonyultak a sugárterápiás kutatás területén.

A kutatásaink során e potenciálisan ígéretes modell besugárzási geometriájának optimalizálása, a halembriók megfelelő elhelyezésére szolgáló eszközök fejlesztése, dozimetriai mérések a kifejlesztett eszközökkel, valamint a besugárzási paraméterek meghatározása történt meg.

Ezt követően a letalitáson kívül egyéb kvantifikálható biológiai végpontokat határozzunk meg (gyulladásos citokinek mértékének vizsgálata, szervi rendellenességek vizsgálata), annak érdekében, hogy lehetségessé váljon különböző sugárminőségek, innovatív sugárforrások, így lézer indukált ionizáló sugárzások tesztelése. Vizsgálataink során gondos dozimetriai méréseket követően különböző posztfertilizációs (hpf) korban lévő (3 hpf, 6 hpf, 24 hpf) vad típusú embriók teljes test besugárzását hajtottuk végre 6 MV konvencionális foton forrással különböző dózis szinteken, melyet követően túlélést, különböző szervi és makro- és mikro-morfológiai rendellenességeket detektáltunk a fejlődő embriókban fénymikroszkóp segítségével. Életkor és dózis-függő elváltozások voltak megfigyelhetőek makroszkópiusan illetve mikroszkópiusan, az azonos nagyságú dózis különbségek esetében. A 6 hpf korban besugárzott embriók esetében az LD<sub>50</sub> érték 15 Gy valamint a 24 hpf korú embriók esetében 20 Gy- nek minősült a konvencionális foton forrással való irradiáció során a 7. megfigyelési napon. A 24 hpf embriók nagyon stabilnak, jól reprodukálhatónak bizonyultak az ionizáló sugárzás hatásainak vizsgálatára és a potenciális sugármódosító anyagok tesztelésére.

## **2. Sugármódosító anyag vizsgálata**

Az ionizáló sugárzás hatásait módosító szelektív sugárvédő anyagot vizsgáltunk a normál szövetek sugárterápiából vagy nukleáris balesetkből adódó károsodásainak kivédése/megelőzése céljából. A foszfatidilkolin deacilált, vízben oldódó származékát, az L-alfa glicerilfoszforilkolin (GPC), alkalmaztuk kísérleteink során. Az eredmények alapján a GPC sugárvédő, illetve gyulladáscsökkentő hatásokat mutatott a zebradánió embrió modellben, jelentősen csökkentve a sugárzás okozta proinflammatorikus aktivációt, az ionizáló sugárzás által kiváltott morfológiai károsodásokat és a letalitást.

A GPC-kezelés lehetséges jövőbeli perspektívának bizonyul a rosszindulatú daganatok sugárkezelése során, javítva a terápiás indexet, azáltal, hogy szelektíven védi az egészséges szöveteket a céltérfogat szomszédságában.

### **3. Nagy LET neutron besugárzással végzett vizsgálatok, különböző neutron energiák Relatív Biológiai Effektivitás meghatározása**

Annak tudatában, hogy a korai életszakaszokban az embriók érzékenyebbek az ionizáló sugárzásra, megállapítottuk, hogy 24 hpf életkor alkalmas megbízható sugárbiológiai vizsgálatokra, és ebben a korban az embriók jól tűrik a sugárforrások miatt változó külső feltételeket. Célunk volt továbbá a 24 hpf embriók használatával az RBE meghatározása különböző forrásokkal keltett neutron sugárzás esetében, reaktor hasadási neutronok valamint ciklotron alapú gyors neutronok hatását referencia foton (LINAC 6 MV foton) nyalábbal összehasonlítva.

A túlélési görbék összehasonlítása során azt találtuk, hogy a biológiai hatékonyság 10-szer magasabb a nagy lineáris energiaátadású termikus neutronoknál és 2,5-szer magasabb a ciklotron által generált gyors neutron sugárzásnál.

Dózis és LET függő szervi rendellenességek (testhossz megrövidülése, gerinc görbülete, fej és szem méretének csökkenése, szívburok ödéma, szikhólyag megnagyobbodása) voltak megfigyelhetőek mikroszkopikusan, valamint szövettani elváltozásokat határoztunk meg a szem, agy, máj, izom és a bélrendszer esetében.

### **4. A protonsugárzás biológiai hatásainak vizsgálata a mélydózis görbe különböző pontjain (plató, a Bragg Peak kiszélesítés közepén (mid-SOBP))**

A proton sugárterápia növekvő alkalmazása és a hosszú távú túlélők számának növekedése alapvető vitát váltott ki a normális szövetek lehetséges hatásairól. A klinikailag alkalmazott általános RBE-értéket csak *in vitro* vizsgálatok eredményezték, míg az *in vivo* kísérletek és a klinikai vizsgálatok ritkák. Törekvéseink fő célja a hatások jellemzése, illetve a plató és a mid-SOBP proton sugárzás hatásainak meghatározása volt klinikai MV foton sugár referenciával.

Az embriók túlélési adatainak alapján,  $1,13 \pm 0,08$  és  $1,20 \pm 0,04$  RBE értékeket határoztunk meg négy nappal a 20 Gy plató és mid-SOBP proton besugárzása után a 6 MV foton forrással való besugárzáshoz viszonyítva. Ezeket az RBE értékeket igazolták az embriók morfológiai rendellenességeinek megjelenésének arányai is, a megfelelő sugárminőségek és dózisok tekintetében.

Összefoglalva, adataink azt mutatták, hogy a zebradánió halembrió rendszer megbízható *in vivo* modellnek bizonyult, mely egy robusztus és egyszerű alternatív modelltként alkalmazható különböző ionizáló sugárzások biológiai hatásainak vizsgálatára, valamint az RBE meghatározására. Nagyszámú

egyed felhasználásával a túlélési arány jól reprodukálható eredményeket mutatott a különböző kezelések esetében.